Thermal Modelling of Meliadine Discovery WRSFs

December 9, 2022

AGNICO EAGLE

okane

Integrated Mine Closure and Relinquishment Solutions

Thermal Modelling of Meliadine Discovery WRSFs

948-229-001 Rev1

December 2022

Prepared for:

Agnico Eagle Mines Limited
11600 rue Louis-Bisson
Mirabel, QC
J7N 1G9

Prepared by:

Gillian Allen
Senior Engineer
gallen@okc-sk.com

Okane Consultants Inc.

112 - 112 Research Drive
Saskatoon, SK S7N 3R3
Canada

Telephone: (306) 955 0702
Facsimile: (306) 955 1596
Web: www.okc-sk.com

Rev. #	Rev. Date	Author	Reviewer	PM Sign-off
0	November 28, 2022	LT	GA	GA
1	December 9, 2022	LT	GA	GA

DISCLAIMER

This document has been provided by Okane Consultants Inc. (Okane) subject to the following limitations:

1. This document has been prepared for the client and for the particular purpose outlined in the Okane proposal and no responsibility is accepted for the use of this document, in whole or in part, in any other contexts or for any other purposes.
2. The scope and the period of operation of the Okane services are described in the Okane proposal and are subject to certain restrictions and limitations set out in the Okane proposal.
3. Okane did not perform a complete assessment of all possible conditions or circumstances that may exist at the site referred to in the Okane proposal. If a service is not expressly indicated, the client should not assume it has been provided. If a matter is not addressed, the client should not assume that any determination has been made by Okane in regards to that matter.
4. Variations in conditions may occur between investigatory locations, and there may be special conditions pertaining to the site which have not been revealed by the investigation, or information provided by the client or a third party and which have not therefore been taken into account in this document.
5. The passage of time will affect the information and assessment provided in this document. The opinions expressed in this document are based on information that existed at the time of the production of this document.
6. The investigations undertaken and services provided by Okane allowed Okane to form no more than an opinion of the actual conditions of the site at the time the site referred to in the Okane proposal was visited and the proposal developed and those investigations and services cannot be used to assess the effect of any subsequent changes in the conditions at the site, or its surroundings, or any subsequent changes in the relevant laws or regulations.
7. The assessments made in this document are based on the conditions indicated from published sources and the investigation and information provided. No warranty is included, either express or implied that the actual conditions will conform exactly to the assessments contained in this document.
8. Where data supplied by the client or third parties, including previous site investigation data, has been used, it has been assumed that the information is correct. No responsibility is accepted by Okane for the completeness or accuracy of the data supplied by the client or third parties.
9. This document is provided solely for use by the client and must be considered to be confidential information. The client agrees not to use, copy, disclose reproduce or make public this document, its contents, or the Okane proposal without the written consent of Okane.
10. Okane accepts no responsibility whatsoever to any party, other than the client, for the use of this document or the information or assessments contained in this document. Any use which a third party makes of this document or the information or assessments contained therein, or any reliance on or decisions made based on this document or the information or assessments contained therein, is the responsibility of that third party.
11. No section or element of this document may be removed from this document, extracted, reproduced, electronically stored or transmitted in any form without the prior written permission of Okane.

EXECUTIVE SUMMARY

The Meliadine Mine is comprised of six known gold deposits and development is proceeding in a phased approach (known as the Approved Project under the Water License Amendment, and the Meliadine Extension), until 2043. The phased approach allows for development to occur within capital constraints and during concurrent exploration. The Meliadine Extension will be composed of 12 additional open pits, for a total of 17 open pits, and underground workings, waste rock storage facilities, tailings storage facilities expansion, water management facilities, and construction of a haul road between Tiriganiaq and Discovery.

Okane Consultants (Okane) was retained by Agnico Eagle Mines Limited (Agnico Eagle) to complete a thermal assessment, which also includes evaluation of seepage conditions, of the Discovery waste rock storage facilities (WRSFs) at the Meliadine Extension. The objectives of the detailed thermal and seepage modelling are to:

- Provide long-term hydrologic and thermal inputs for the site-wide water and load balances for assessing the impact of the WRSF on site-wide water quality; and
- Support a basis for closure design of the WRSF, which is defendable to internal project stakeholders and regulators.

The Discovery WRSFs are expected to have a much smaller proportion of overburden compared to other Meliadine WRSFs. In addition, most of the waste rock planned for the Discovery WRSFs is expected to be classified as being 'uncertain' with respect to acid generating potential or be potentially acid generating and/or metal leaching (PAG/ML) (Golder, 2014a). An updated waste rock characterization study completed by Lorax (2022) was subsequently completed to increase the level of confidence in the distribution of PAG/ML and NPAG/NML waste rock. Due to the larger proportion of PAG/ML waste rock at the Discovery WRSFs, a 6 m non-potentially acid generating and/or non-metal leaching (NPAG/NML) waste rock cover system has been proposed for closure to limit interaction of precipitation with PAG/ML material to the extent necessary to be protective of water quality. For the purpose of modelling presented herein, it was assumed that all waste rock beyond the 6 m cover system at Discovery WRSFs is PAG/ML. It is acknowledged that the assumption that all waste rock is PAG/ML is a 'bookend' perspective with respect to potential influence of the presence of PAG/ML material within the Discovery WRSFs, and that this assumption must be retained for the moment and revisited in the future once additional information with respect to waste rock composition, volumes, and schedule is developed.

A climate change scenario was modelled, Representative Concentration Pathway (RCP) 4.5, consistent with permitted conditions for the existing Meliadine project. RCP4.5 represents a 'medium RCP' scenario with stabilization of radiative forcing around 2100. RCP4.5 has been selected as the base case condition for the extension project. RCP4.5 predicts an average annual temperature of approximately -4.6 °C over

the last 30 years of the climate change database (2090-2120) compared to the current average of -10.4 °C based on the historical climate database (1981-2020).

The Discovery WRSFs are expected to have high surface infiltration capacity as a result of the physical nature of the waste rock (i.e., the coarser-textured nature). This high infiltration capacity is expected to lead to formation of ground ice at the boundary of the active layer over time. As this ice layer is established, infiltration will gradually be diverted laterally along the ice layer within the active zone, resulting in interflow reporting at the toe of the WRSFs. Interflow occurs as unsaturated flow, and thus has a long transit time for water infiltrating near the top of the WRSFs. This transit time is in the order of decades, so WRSFs will take decades to reach a pseudo steady-state hydrologic condition where most net surface infiltration reports as interflow.

The hydrologic condition described above is influenced by the depth of the active layer, which dictates the expected location of the ice layer. The majority of interflow occurs along the boundary of the ice layer which maintains pore air temperatures less than 2 °C year-round. The active layer is expected to reach up to 6 m under RCP4.5 conditions, reducing the likelihood of any interaction between infiltration beyond the proposed cover system. The increased active layer depth at Discovery, compared to the Meliadine WRSFs is the result of heating from exothermic reactions from the oxidation of PAG/ML waste rock. The modelled scenario is assumed to be conservative as all waste rock has considered to be PAG/ML.

TABLE OF CONTENTS

LIST OF TABLES

LIST OF FIGURES

1 INTRODUCTION

Agnico Eagle Mines Limited (Agnico Eagle) operates the Meliadine Mine, located approximately 25 km north of Rankin Inlet, and 80 km southwest of the hamlet of Chesterfield Inlet in the Kivalliq Region of Nunavut. The Meliadine Mine was approved to proceed subject to Terms and Conditions of the Project Certificate No. 006. The Project is composed of six known gold deposits: Tiriganiaq, F Zone, Pump, Wesmeg, Wesmeg North, and Discovery, with approval to mine all deposits using open pit methods, and to mine Tiriganiaq with open pit and underground methods. Approved facilities include ore stockpiles, waste rock storage facilities, a tailings storage facility, and other various infrastructure.

Agnico Eagle is proposing to expand the Mine (referred to as the Meliadine Extension) through additional underground mining and open pit mining. The Meliadine Extension is proceeding in a phased approach until 2043. The phased approach allows for development to occur within capital constraints and during concurrent exploration. The Meliadine Extension will be composed of 12 additional open pits, for a total of 17 open pits, and underground workings, waste rock storage facilities, a tailings storage facility expansion, water management facilities, and construction of a haul road between Tiriganiaq and Discovery. Okane Consultants (Okane) was retained by Agnico Eagle to complete a water balance assessment of the waste rock storage facilities (WRSFs) to support development of the Meliadine Extension Project for regulatory approval.

Thermal modelling will assist in developing an understanding of the expected seasonal active layer through operations and post-closure and determine if permafrost conditions within the WRSFs are sustainable under climate change conditions. As part of this objective, a landform water balance was also completed for the operational, closure and post closure phases, including estimates of runoff, interflow, and basal seepage rates. Results of this thermal and seepage modeling work will be used to meet requirements of the impact statement guidelines, and to inform other work such as a detailed site water quality and load balance model for operations through post-closure.

Assessment of long-term thermal stability waste rock storage, ore storage, and tailings storage was a requirement of the initial environmental impact statement and will be a requirement for any future amendments to the environmental impact statement, the Project Certificate and Water License Amendment.

1.1 Project Objectives and Scope

The objective of the detailed thermal and seepage modelling is to provide long-term hydrologic and thermal inputs for the site-wide water and load balances, as well as a basis for closure design of the WRSFs that it is defendable to internal project stakeholders and regulators.

Based on this objective, the specific deliverables for the modelling program are:

- Estimates of runoff, interflow, and basal seepage from WRSFs and overburden piles under climate change conditions scenarios agreed upon by Agnico Eagle.

- Estimated depths of interaction and pore space temperatures for runoff, interflow, and basal seepage from the WRSFs and overburden piles under climate change conditions scenarios agreed upon by Agnico Eagle.

1.2 Report Organization

For convenient reference, this report has been subdivided into the following sections:

- Section 2 – Provides a summary of the site background and a conceptual model of performance of the proposed WRSFs at Meliadine;

- Section 3 – Presents the model assumptions and inputs used for the numerical modelling simulations completed;

- Section 4 – Summarizes the results of the numerical models and provides a discussion on the potential implications of results on site-wide water quality; and

- Section 5 - Analyses the results in the context of the stated objectives of the modelling program.

2 BACKGROUND

The Meliadine Extension includes 12 additional open pits (for a total of 17 open pits) and underground workings, WRSFs, tailings storage facility expansion, water management facilities, and construction of a haul road between Tiriganiaq and Discovery (Figure 2.1 and Figure 2.2).

Waste rock and overburden will be trucked to WRSFs throughout mine operations. Currently, the Approved Project is in operation with development of the Tiriganiaq Underground deposit and construction of WRSF1 and WRSF3. At both facilities, overburden will be encapsulated by waste rock. It is assumed that similar construction methodology will form the base case for the Meliadine Extension WRSFs.

Waste generation from mining at the Discovery site are scheduled to begin in 2031. Two WRSFs (WRSF8 and WRSF9) will be constructed to manage waste from the Discovery open pit.

Initial investigations of the Discovery waste rock indicated the potential for higher acid rock drainage (ARD) potential and therefore a 6 m surface layer of non-potentially acid generating and non-metal leaching (NPAG/NML) waste rock, intended to limit thaw of potentially acid generating and metal leaching (PAG/ML), has been proposed as a closure cover system.

2.1 Conceptual Model

A conceptual model describes key processes, or mechanisms, and their site-specific respective controls, which are expected to influence performance of the proposed WRSFs. It is presented at a conceptual level, using a hierarchy of climate, geology and materials, and topography, leading to an understanding of the patterns of water movement on a specific landscape (INAP, 2017).

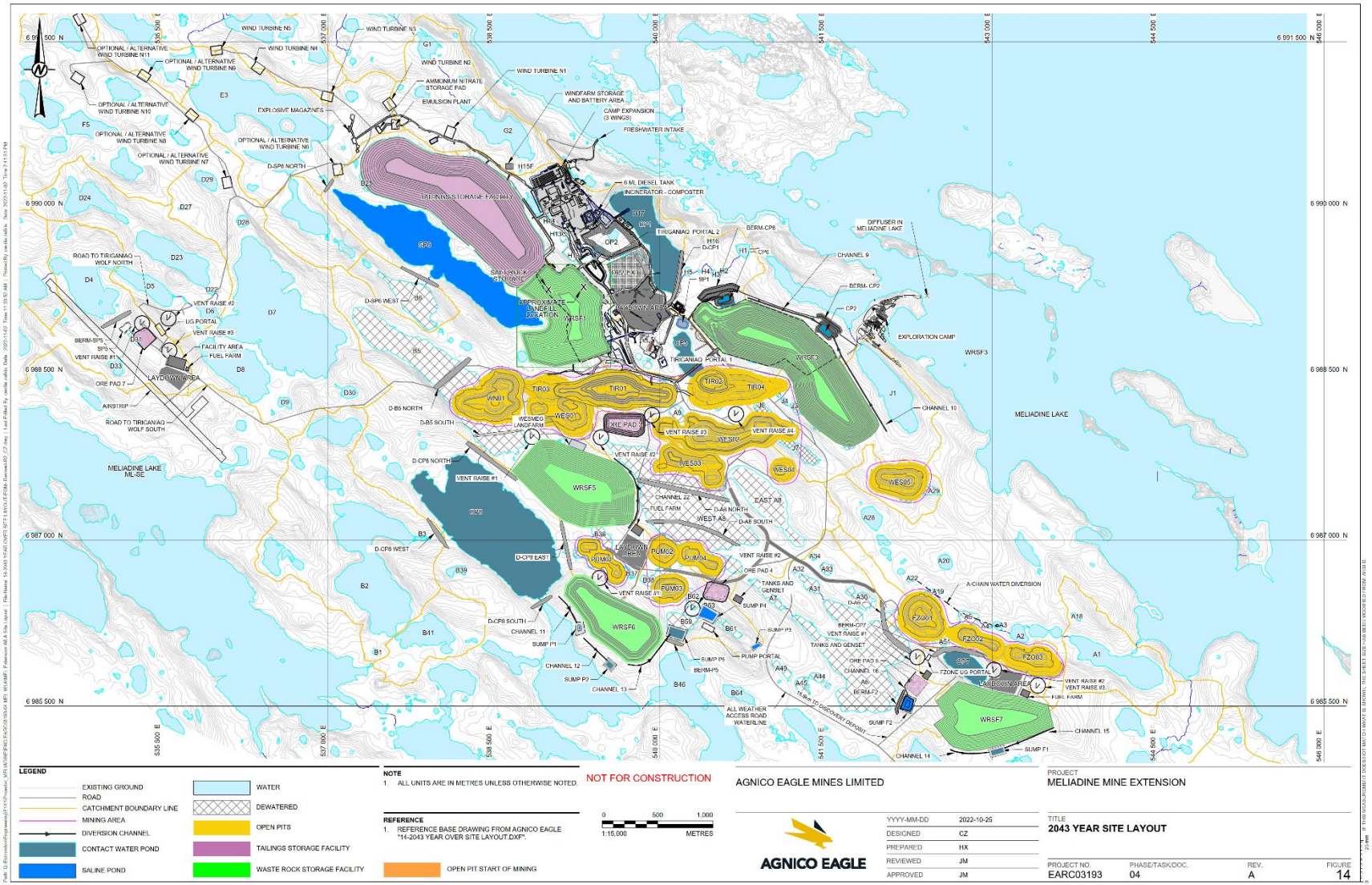

Figure 2.1 : Meliadine Extension site layout.

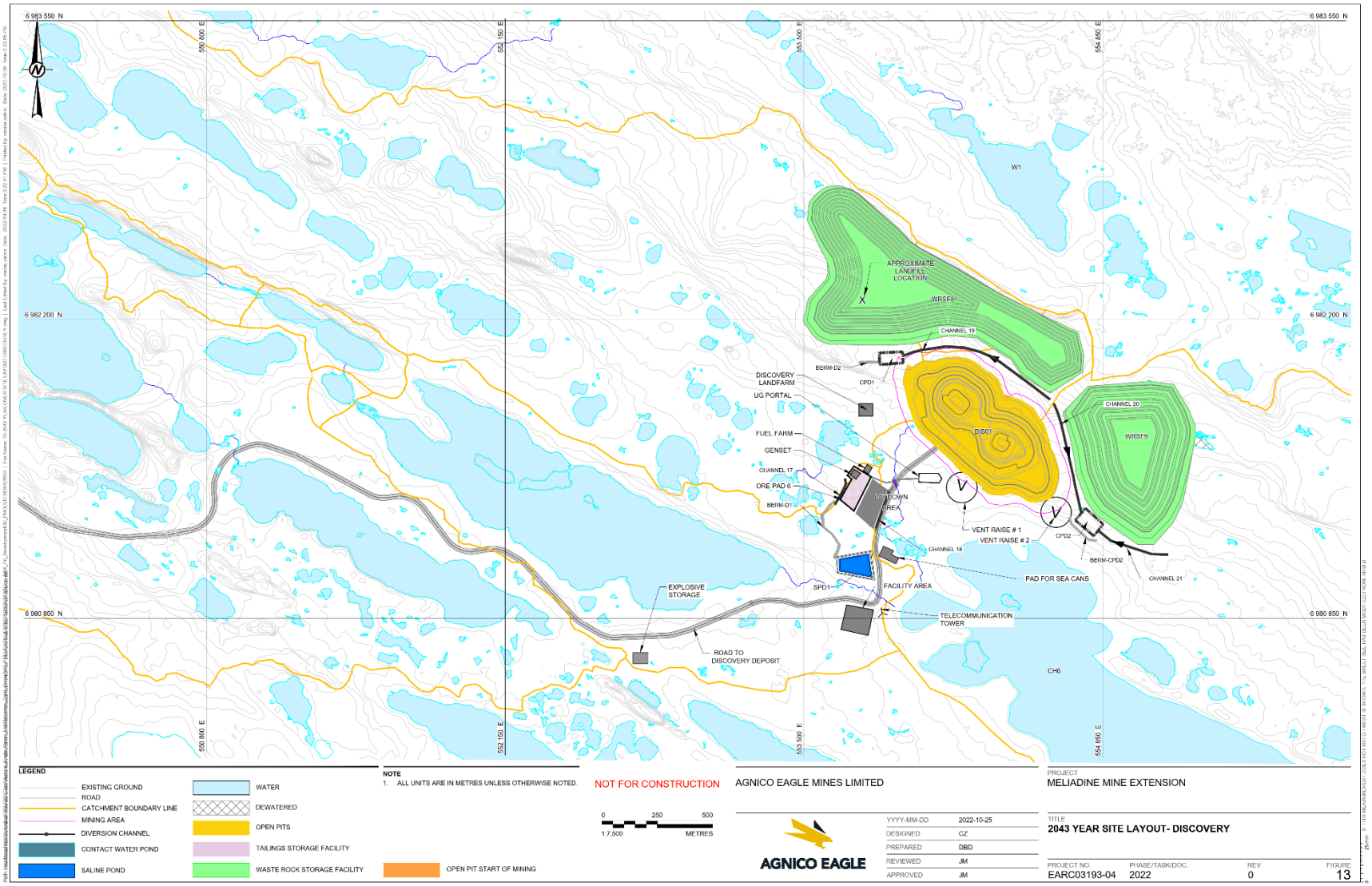

Figure 2.2: Meliadine Discovery site layout.

2.1.1 Conceptual Model of Surface Water Balance

The Meliadine site falls near the intersection of the ET (polar tundra) and Dfc (subarctic climate) classification of the Köppen-Geiger climate classification system where:

- E – 'polar' where average temperature of the warmest month is < 10 °C;
- T – 'tundra' where the average temperature of the warmest month is < 10 °C, but > 0 °C;
- D – 'continental' where average temperature of the coolest month is < -3 °C, and average temperature of warmest month > 10 °C;
- f – 'without a dry season' where precipitation is relatively evenly distributed throughout the year; and
- c – 'cold summer' where one to three months average temperature reach < 22 °C but > 10 °C.

Annual precipitation is approximately 430 mm, distributed relatively evenly as snowfall and rainfall. Climate data suggest that the site has a relatively balanced annual surface water budget, or slight water deficit, where the ratio of potential evapotranspiration (PET), sublimation, and snow redistribution is approximately equal to total annual precipitation. There is expected to be a water deficit throughout the summer as potential evaporation (PE) exceeds rainfall in June through August, and a water surplus in September, as PE decreases. Climate data suggest that net percolation, the water that moves from a cover system into a WRSF when a cover system is in place, or simply just surface infiltration when there is no cover system placed, is likely to occur in the fall period when PE is low, and potentially during spring freshet.

Waste rock is expected to have very low available water holding capacity (AWHC) (<3 mm). The available water holding capacity refers to the volume of water held within a granular material that may be available for evapotranspiration. Given high evaporative conditions in July through August, this available water holding volume may be 'recycled' several times, as the volume of water held in the waste rock increases following a rainfall event, then is evapotranspired in the following period when it is no longer raining (or evaporates if/when there is little to no vegetation present). Climate data indicates there are typically 50-60 days where precipitation occurs between July to August. Based on the assumption that evapotranspiration is limited to non-rainfall days and is limited to the surficial metre of material, the maximum probable volume of water lost to evapotranspiration is approximately between 55 mm to 165 mm. This depth of evapotranspiration represents roughly 15%-40% of total annual precipitation.

The coarser-textured nature of the waste rock, which results in low available water holding capacity, also results in high surface infiltration capacity (though influenced by non-frozen conditions), and thus low surface water runoff potential. In short, the potential for saturated overland flow is very low. As noted,

frozen conditions in the waste rock during spring freshet will both decrease the permeability of the waste rock and reduce viscosity of the water as it approaches its freezing point, leading to the potential for a small volume of runoff to occur in the freshet period.

The last parameter influencing surface infiltration is the portion of snowfall that is sublimated or redistributed. Conditions for sublimation and redistribution are high at Meliadine, particularly at the WRSFs, where windspeed is high and WRSFs are the predominant feature within the landscape. The potential for redistribution is expected to result in a net loss of snow on the WRSF (without accounting for sublimation). Previous estimates (Golder, 2014b) indicated that sublimation may account for up to 50% of the total winter precipitation, or 25% of total annual precipitation. This proportion may be even higher for the wind blown WRSFs at Meliadine.

Given the above drivers of the surface water balance, surface infiltration into the WRSF is expected to be 'high', between approximately 30% to 50% of total annual precipitation (130 mm to 215 mm). Given the low AWHC of the waste rock, the time for wet up of the landform is expected to be relatively short, as the *in-situ* water content of the waste rock is likely similar to its drained field capacity. However, the permafrost conditions which exist within the WRSF will allow for additional water to be stored in the waste rock beyond its field capacity. Fully saturated ice zones are expected to form along the boundary of the seasonal active layer, creating a low permeability ice zone. The active layer in the Meliadine area is generally between 1.0 m to 3.0 m (Golder, 2014b); however, the active layer is expected to be deeper in the WRSF as the thermal conductivity of waste rock is higher, and the volumetric heat capacity is lower than surrounding surficial overburden. The formation of a low permeability ice zone is anticipated to occur in the order of decades.

The presence of a lower permeability ice zone coupled with the lower permeability of *in situ* surficial overburden and waste overburden or waste rock is expected to reduce basal seepage to negligible levels.

Once the lower permeability ice zone has formed, the WRSF will largely reach a pseudo steady-state condition where, from a hydraulic performance perspective, net surface infiltration will report as toe seepage (or interflow along the lower permeability ice zone) from the WRSF (Figure 2.3). This, however, should not be interpreted as a 'plug flow' condition, where a drop of water infiltrating on the plateau of the WRSF reports as interflow in the same time frame as a drop of water infiltrating near the toe of the WRSF. The 'age' of interflow observed will increase over time as areas further away from the toe begin to report, finally reaching a pseudo 'steady-state' condition from a geochemical perspective. This process is also expected to occur in the order of decades. Lastly, interflow water quality is expected to evolve over the life of mine as buffering capacity of PAG/ML waste rock may be exceeded, and available reactive minerals are slowly exhausted.

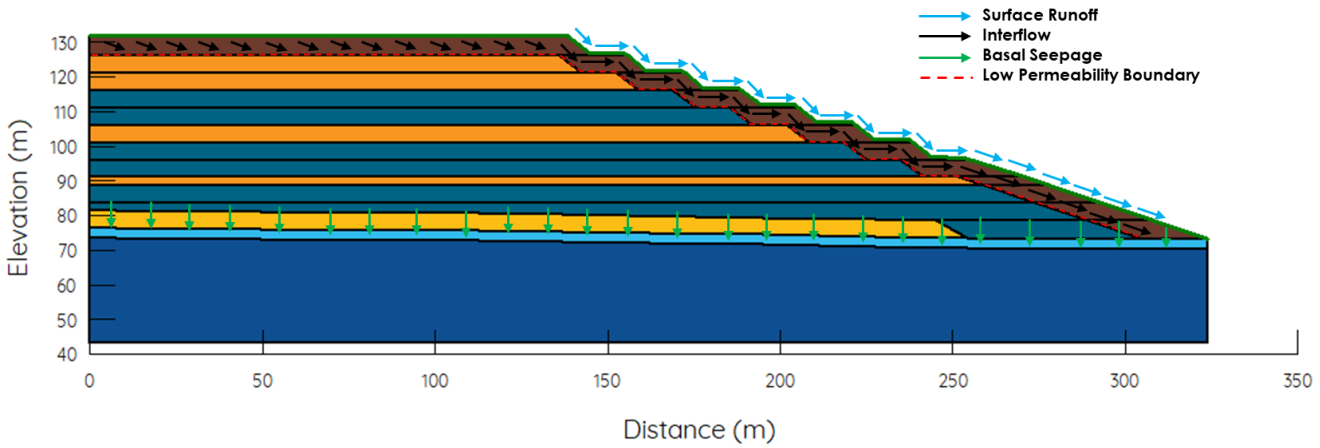

Figure 2.3: Conceptual sketch of landform water balance at Meliadine WRSFs.

Climate change in the region is expected to result in a warmer and wetter climate. The anticipated rise in average annual temperature is likely to increase the thickness of the active layer, potentially thawing a portion of the lower permeability ice layer already in place or increasing its depth within the WRSF. The increase in temperature is likely also to increase evaporative conditions; however, this is expected to be similar in proportion to the increase in precipitation resulting in a similar proportion reporting as net percolation (and surface infiltration).

2.1.2 Conceptual Model for Oxygen Ingress

Oxygen availability throughout the WRSFs is not expected to be limited in the short term as the waste rock has very high air permeability (coarser-textured material of relatively low water content when placed). Air permeability can be estimated based on the intrinsic permeability derived from the estimated hydraulic conductivity for a given material, which can be measured in laboratory, or estimated based on material texture (Fredlund *et al*., 2012). The waste overburden, however, has much lower air permeability. However, given the minimal overburden present within the core of the Meliadine Discovery WRSFs it is not expected to limit formation of large-scale convective airflow cells, which are known to encourage freezing of coarser-textured WRSFs in cold climates (Pham *et. al*, 2013). While co-disposal may limit convective cooling, it is not expected to inhibit freeze-back given the current climate at Meliadine. The lower air permeability of the waste overburden, however, is not expected to limit oxygen availability, as the overburden is assumed to have low reactivity (i.e. the consumption of oxygen due to oxidation reactions in the waste overburden is likely lower than the air permeability).

The presence of ice zones at the boundary of the active layer are expected to reduce air permeability over time. This may delay freeze back of the WRSFs.

2.2 Description of Numerical Modelling Program

GeoStudio Version 11 was used to conduct the modelling for this project, the same software and version that was used in the Whale Tail and IVR WRSFs thermal modelling. This version of GeoStudio is a substantial upgrade to previous software versions, as it accounts for advective air flow as well as mineral oxidation within the WRSF and associated heat generation via an add-in module developed for the software. Four components of the GeoStudio suite of programs were used in combination for this project: SEEP/W; TEMP/W; AIR/W, and CTRAN/W (with the gas consumption and exothermic reactions add-in incorporated into the CTRAN analysis).

SEEP/W is a 1D/2D finite element model that can be used to model the saturated and unsaturated movement of moisture and pore-water pressure distribution within porous materials such as soil and rock. The latest version of SEEP/W incorporates a module that allows for soil-plant-atmosphere (SPA) modelling that was previously included in a separate software package (VADOSE/W). This module calculates pressure head (suction) and temperature profiles in the material profile in response to climatic forcing (such as evaporation) and lower boundary conditions (such as a water table). A key feature of the module is the ability of the model to determine actual evaporation and transpiration based on potential evaporation and predicted suction, as opposed to the user being required to input these surface flux boundary conditions. The actual evapotranspiration rate is generally well below the potential rate during prolonged dry periods because the suction in the material profile increases as the surface desiccates. In addition, the module is a fully coupled (through the vapour pressure term) heat and mass transfer model that is capable of simulating water vapour movement.

The SPA model of SEEP/W is also capable of evaluating the impact of frozen conditions on moisture storage and transport for a given soil or rock material. The change of phase from liquid to solid (i.e. water to ice) is accounted for using the apparent specific heat capacity approach, standard in thermal modelling. A heat source or sink is added at each time step based on the amount of heat released when a set volume of water changes to ice. When the ground becomes frozen, the permeability must be reduced. In the physics of freezing, there is a phenomenon whereby even in a saturated material, a "suction" develops at the ice-water interface much like that at the air-water interface in an unsaturated soil. If the temperature below freezing is known, then the suction can be computed using the Clausius Clapeyron phase equilibrium equation (Black and Tice, 1989). The SPA module does not account for this suction at the microscopic level in the mass transfer equation but does use the actual temperature to compute what the suction should be so that the program can look up a reduced permeability from the material's hydraulic conductivity function (suction versus hydraulic conductivity). SEEP/W simulations can be completed with or without this functionality.

TEMP/W is a 1D/2D finite element model that can be used to model thermal changes in porous systems due to various changes in the environment, internal changes in temperature, or any other influencing condition that may result in a change of temperature in the subsurface. Typically, in a TEMP/W simulation, it is assumed that moisture content remains the same. However, when water movement occurs in a

system, substantial heat transfer can occur as a result of this movement of water. As such, by coupling the TEMP/W simulation with a SEEP/W simulation, a more accurate temperature condition in the subsurface can be estimated. The freezing point depression caused by increased salinity can be considered in TEMP/W through the phase change temperature and the unfrozen water content function. Adjusting the unfrozen water content function has the advantage of being material specific, but without adjusting the phase change temperature, the latent heat is still applied at 0 °C rather than the freezing point depression. Adjusting the phase change temperature affects the entire model domain, which may not be ideal for situations where not all porewater is saline.

AIR/W is a 2D finite element model that is executed within the SEEP/W model, which can be used to model air pressure and flow within a system in response to changes in pressure conditions at the boundary, or changes in water pressure. When coupled with TEMP/W, it can also calculate changes in air flow and pressure as a result of changes in air temperature.

CTRAN/W, with the addition of the gas consumption and exothermic reactions add-in, couples the gas, heat, water, and air transfer processes to simulate the exothermic oxidation process. The add-in models the oxidation process as an irreversible first order reaction. The rate of reaction is dependent on, and controlled by, the availability of oxygen, as well as temperature. The add-in allows oxygen to be consumed and heat to be produced within the WRSF due to sulphide oxidation. The current version of the add-in does not take into account mineral depletion with time, and thus assumes there is a constant supply of sulphide to oxidize, resulting in a conservative estimate of the heat added to the domain as a result of the exothermic oxidation process.

3 MODEL INPUTS

Model inputs for Meliadine Discovery WRSFs can be divided into five types:

1) Climate / Upper Boundary Conditions;
2) Materials;
3) Geometry;
4) Lower and Edge Boundary Conditions; and
5) Initial Conditions.

The following sections describe the inputs used.

3.1 Climate

TEMP/W, SEEP/W, and AIR/W require daily values of: maximum and minimum air temperature; maximum and minimum relative humidity (RH); average wind speed; daily net radiation; and precipitation (amount and duration). Historical values for all these parameters, except net radiation, are available from Environment and Climate Change Canada (ECCC) for Rankin Inlet (Station ID: 2303405 and 2303401) (ECCC, 2020), approximately 25 km south of the Meliadine site. Solar radiation for Rankin Inlet is estimated by Environment and Climate Change Canada in the Canadian Weather Energy and Engineering Datasets (CWEEDS) using the MAC3 model (ECCC, 2016). This data was used to estimate net radiation on a daily basis. ECCC has hourly records for Rankin Inlet from 1981 to present, of which the period January 1981 to January 2020 was used to create a 39-year database for the Meliadine WRSFs. ECCC also provides precipitation data that have been adjusted for gauge undercatch and evaporation due to wind effect, which was incorporated into the Meliadine climate database (ECCC, 2017). The adjusted precipitation data is available until 2013, after which the methodology was reproduced by Tetra Tech (2021) and applied to subsequent years. After comparing the climate data measured at Meliadine from October 2014 to December 2019 to measurements taken at Rankin Inlet for the same time period, it was concluded that the Rankin Inlet data did not need to be adjusted to represent the Meliadine site. Any missing data in the Rankin Inlet climate record were filled with average measurements for a given day.

Table 3.1 provides a summary of the average monthly conditions in the 39-year historical database developed for the Meliadine Mine.

Table 3.1: Summary of average climate parameters for the 39-year Meliadine historical climate database with Tetra Tech (2021) adjusted precipitation.

Month	Temperature (°C)		Relative Humidity (%)		Wind (m/s)	Net Radiation[1] (MJ/m²/day)	Precipitation	
	Maximum	Minimum	Maximum	Minimum			(mm)	(days)
January	-26.7	-33.9	75.3	68.4	6.7	-1.8	17	27
February	-26.4	-33.7	81.8	71.2	6.6	-1.0	17	25
March	-20.7	-29.2	86.8	74.3	6.5	0.1	22	27
April	-11.4	-20.4	94.2	74.9	6.3	2.5	29	22
May	-2.3	-8.9	93.3	65.7	6.2	5.0	30	21
June	8.1	0.6	94.2	69.4	5.6	7.2	32	15
July	15.1	6.3	93.5	67.0	5.4	8.0	46	16
August	13.2	6.3	94.1	81.1	5.9	5.5	59	18
September	6.4	1.4	85.0	77.7	6.6	2.3	53	21
October	-1.8	-7.2	79.8	72.8	7.3	-0.1	57	27
November	-13.0	-20.8	75.2	69.8	6.9	-2.0	39	27
December	-21.7	-29.2	71.8	66.4	6.6	-2.2	25	28
Annual	-6.7	-14.0	83.0	71.3	6.4	1.9	426	272

[1] Net radiation for a level location (e.g. the plateau of the WRSF)

A "synthetic average" climate year was defined by averaging the daily climate conditions from the 39-year climate database (e.g., averaging the maximum temperature on January 1st for all 39 years). However, precipitation was not applied considering solely the daily average amount, but also the average number of precipitation events per month. Hence, precipitation was applied for the average number of rainfall days per month and on days with the highest chance of rainfall. The daily rainfall amounts for days with lower chances of rainfall were added to the next high-chance event in the month so that the synthetic average climate year had the average amount of rainfall.

3.1.1 Climate Change

The 39-year historical database presented above was adapted to account for climate change predictions over the next 100 years. This process is explained in the remainder of this section.

As part of the Intergovernmental Panel on Climate Change's (IPCC) Fifth Assessment Report (AR5), the IPCC adopted new representative concentration pathways (RCPs) to replace the previous emission scenarios of the Special Report on Emission Scenarios (SRES) (IPCC, 2013). The four adopted RCPs differ from the SRES in that they represent greenhouse gas concentration trajectories, not emissions trajectories. The four scenarios (RCP2.6, RCP4.5, RCP6.0 and RCP8.5) are named after the radiative target forcing level for 2100, which are based on the forcing of greenhouse gases and other agents and are relative to pre-industrial levels (van Vuuren *et al.*, 2011). RCP2.6 represents a very low RCP with a peak of

radiative forcing at around 3.1 W/m^2 mid-century, followed by a decline to 2.6 W/m^2 by 2100. RCP4.5 represents a medium RCP with stabilization of radiative forcing around 2100. RCP6.0 represents a medium-high RCP with stabilization of radiative forcing shortly after 2100, while RCP8.5 represents a high RCP with increasing emissions that do no stabilize until after 2200. Climate at the Meliadine site is expected to remain within the subarctic (Dfc) climate category, described above, under the A1FI (former SRES emission scenarios) climate change scenario, which is similar to RCP8.5 (Rubel and Kottek, 2010). A 100-year climate change database for this project was developed using daily data under RCP4.5, RCP6.0 and RCP8.5. Figure 3.1 provides the concentration of all forcing agents (in parts per million (ppm) of CO_2-equivalence) for the four RCP scenarios.

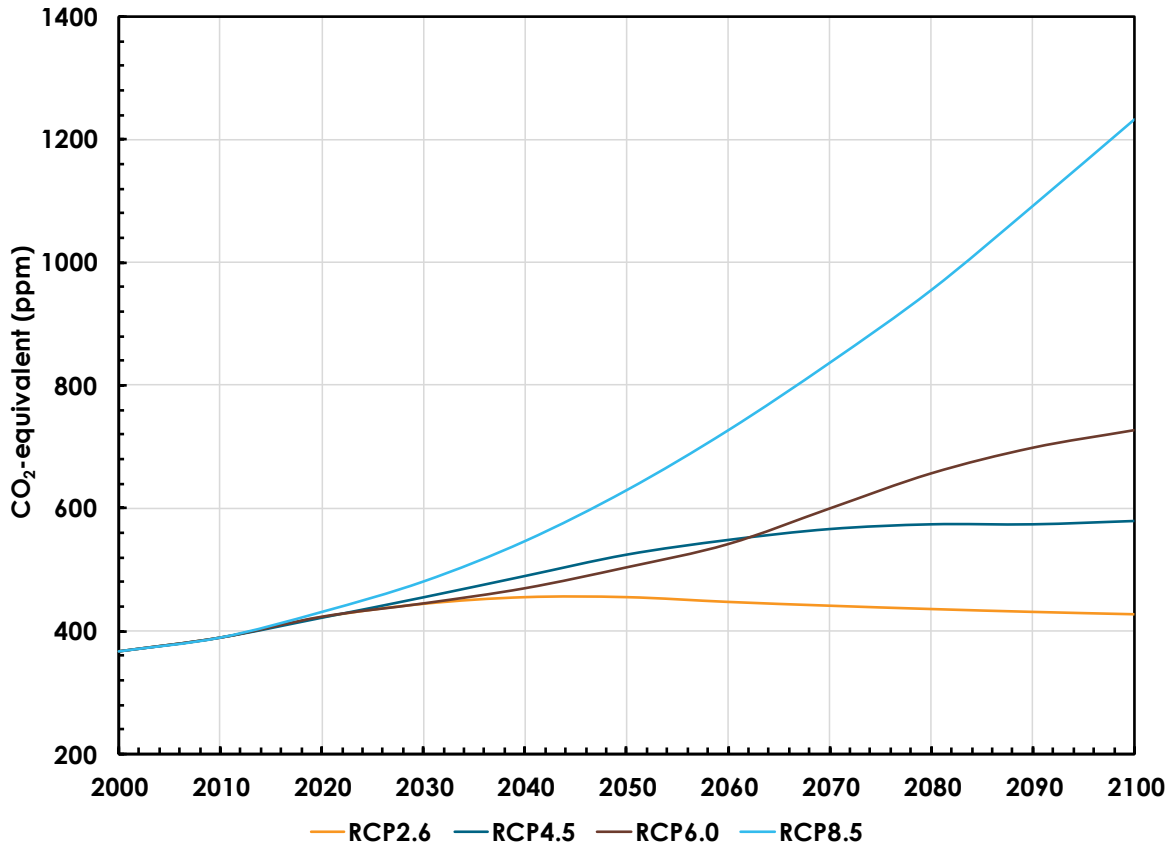

Figure 3.1: All forcing agents' atmospheric CO_2-equivalent concentrations according to the four RCP scenarios.

The climate change database for Meliadine was developed following the recommendations outlined on the Canadian Climate Data and Scenarios (CCDS) website, which is wholly supported by ECCC (CCDS, 2018). The website recommends the use of statistical downscaling to "downscale" a general circulation model's (GCM's) predictions to a specific location based on historical observations. Statistical downscaling is a two-step process consisting of: i) development of statistical relationships between local climate variables (e.g., surface air temperature and precipitation) and large-scale predictors (e.g., pressure fields), and ii) application of such relationships to the output of GCM experiments to simulate

local climate characteristics in the future. The Pacific Climate Impact Consortium (PCIC) at the University of Victoria provides statistically downscaled daily temperature and precipitation under the RCP2.6, RCP4.5 and RCP8.5 scenarios for all of Canada at a resolution of approximately 10 km (PCIC, 2018). For this project, the second-generation Canadian Earth System Model (CanESM2), developed by the Canadian Centre for Climate Modelling and Analysis (CCCma), was used as the predictor GCM to downscale and make climate change databases representative of Meliadine. Temperature and precipitation were derived from the PCIC output, while the other climate variables required for SEEP/W and TEMP/W (i.e. relative humidity and net radiation) were downscaled using the Statistical Downscaling Model (SDSM) (Wilby *et al*., 2002; 2013; 2014), with the exception of wind speed due to the lack of climate change predictors.

Statistical downscaling is limited by the availability of large-scale predictors. Current CCCma CanESM2 model runs are limited temporally to 2100. In order to predict beyond 2100, the radiative forcing trend was applied to the temperature. RCP4.5 and RCP6.0 are expected to stabilize shortly after 2100, while RCP8.5 is expected to continue along the same trend until after 2200 (Meinshausen *et al*., 2011).

RCP4.5 was selected as the scenario for the base case. Figure 3.2 and Figure 3.3 show the annual temperature and precipitation, respectively, estimated for the RCP4.5 100-year climate database developed for Meliadine. Monthly averages for the database are detailed in Table 3.2. Temperatures are anticipated to rise at a rate of approximately 0.06 °C/year for RCP4.5 until approximately 2070, after which there is a reduction in the temperature increase rate. RCP4.5 predicts an average annual temperature of approximately -4.6 °C over the last 30 years of the climate change database (2090-2120). The RCP4.5 scenario also predicts an increase in precipitation with time, with a projected increase of approximately 13 mm over 100 years or 0.013 mm/year.

Previous projections of climate change at Meliadine were completed in support of the Final Environmental Impact Statement (FEIS) (Golder, 2014b). For the 2071-2100 time period FEIS climate change projections were much cooler and drier than the projected values developed for this assessment. The FEIS climate projections were based on emission scenarios of the SRES reported by the IPCC (discussed above) which have since been updated. The previous projections also relied on historic climate records from Baker Lake, as opposed to Rankin Inlet. A comparison of the post-closure climate change projections is provided in Table 3.3.

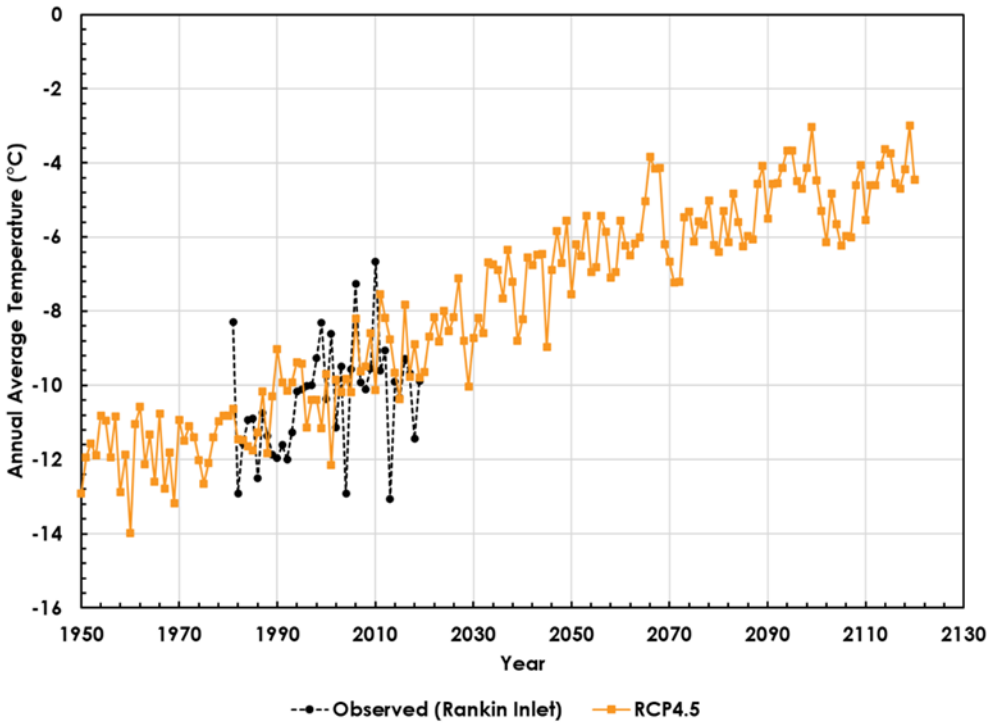

Figure 3.2: Annual average temperature estimated for the RCP4.5 climate change scenario. Observed temperature at Rankin Inlet is also shown.

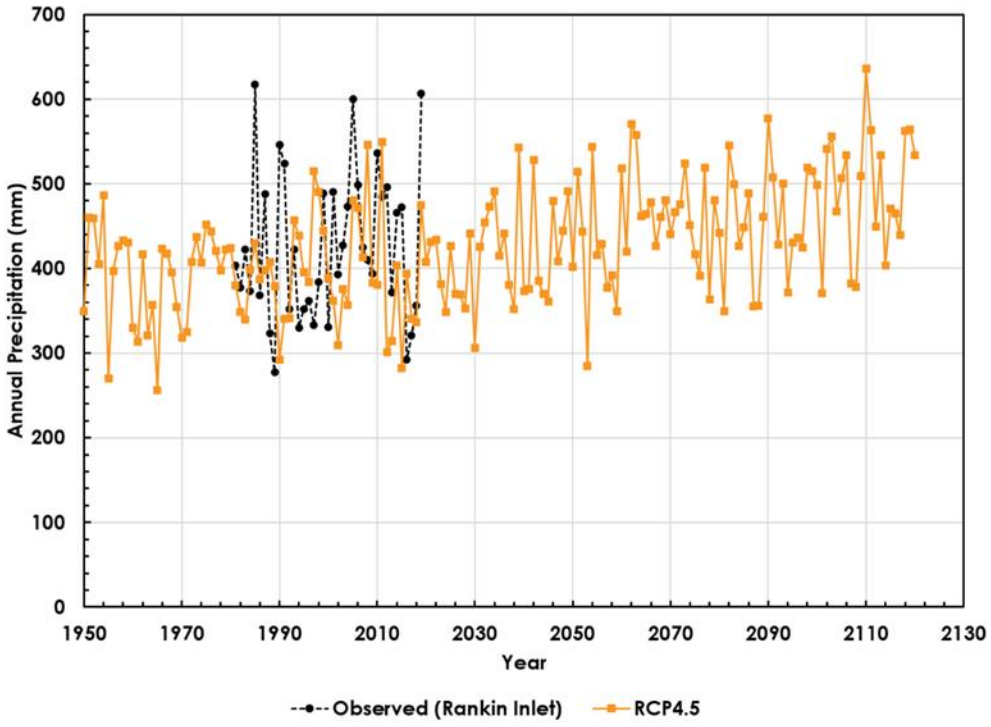

Figure 3.3: Annual precipitation estimated for the RCP4.5 climate change scenario. Observed precipitation at Rankin Inlet is also shown.

Table 3.2: Summary of average climate parameters for the Meliadine climate change database for RCP4.5 (2025-2120)

Month	Temperature (°C)		Relative Humidity (%)		Wind (m/s)	Net Radiation[1] (MJ/m²/day)	Precipitation	
	Maximum	Minimum	Maximum	Minimum			(mm)	(days)
January	-19.4	-26.6	73.4	61.2	6.6	-2.1	24	18
February	-19.6	-26.9	75.4	61.6	6.9	-1.4	20	15
March	-15.8	-23.7	82.2	65.7	6.5	-0.2	27	17
April	-8.8	-16.7	90.7	74.0	6.4	1.6	27	15
May	0.7	-5.3	92.9	71.0	6.3	3.6	28	17
June	13.3	4.8	92.5	59.2	5.9	9.2	31	11
July	17.8	9.3	93.8	61.3	5.4	8.8	48	14
August	15.1	8.8	95.3	67.8	5.6	5.3	58	18
September	8.0	3.2	94.3	72.8	6.2	1.8	61	23
October	0.8	-4.1	90.2	73.9	7.2	-0.6	55	21
November	-8.4	-14.5	81.2	66.1	7.1	-1.8	37	20
December	-14.5	-20.8	74.8	61.9	6.8	-2.1	37	25
Annual	-2.6	-9.4	86.4	66.4	6.4	1.9	452	213

[1] Net radiation for a level location (e.g. the plateau of the WRSF)

Table 3.3: Comparison of FEIS climate projections to current climate projections.

Climate Parameter	2014 FEIS Projection[1]	2022 FEIS Projection RCP4.5[2]
Annual Precipitation (mm)	300.0 to 320.0	455.7
Mean Annual Air Temperature (°C)	-6.7 to -6.2	-5.2

[1] - Golder, 2014b

[2] – Agnico Eagle, 2022

To account for creation of micro-climates on WRSF embankments, calibrations to the base 100-year climate database were done to the net radiation and wind speed parameters. Net radiation was adjusted for north facing and south facing according to the method proposed by Swift (1976) and Weeks and Wilson (2006). Wind direction and speed were also adjusted for the modelled cross sections by creating a specific wind speed data set for NW and SW directions according to the wind roses shown in Figure 3.4 prepared from hourly wind speed and direction data from Rankin Inlet between January 1981 and January 2020. Figure 3.5 shows the wind roses for wind speed and direction from Meliadine Site between September 2014 and December 2019. The effects of surrounding landforms (such as the WRSFs) were assumed not to affect wind speed and direction. As the WRSFs are expected to be the dominant landform in the adjacent landscape, this is a reasonable assumption.

The impact of wind on the thermal regime (forced convection/advection) is likely limited to the edges of the WRSF in the predominant wind direction (NW), as the permeabilities of the materials are not sufficient to allow high enough air velocities within the centre of the WRSF to drive advection (Pham *et al.*, 2015).

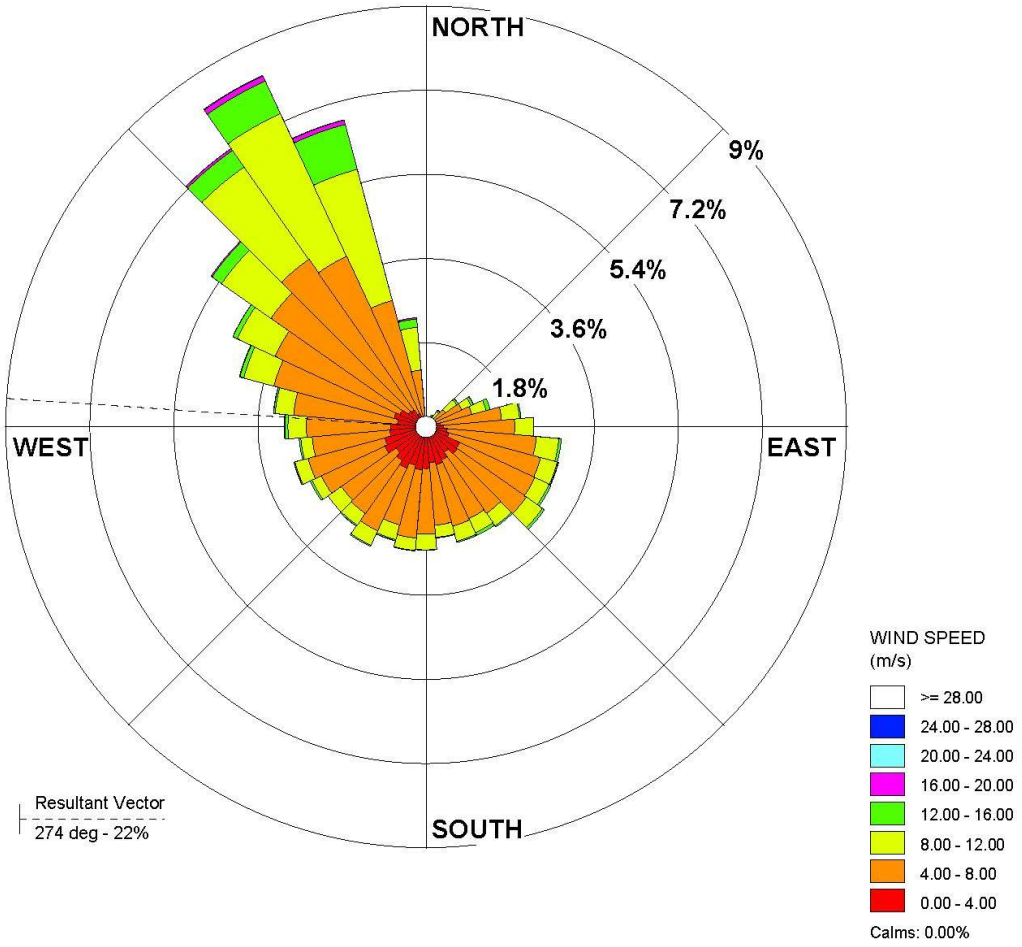

Figure 3.4: Wind rose for Rankin Inlet climate station.

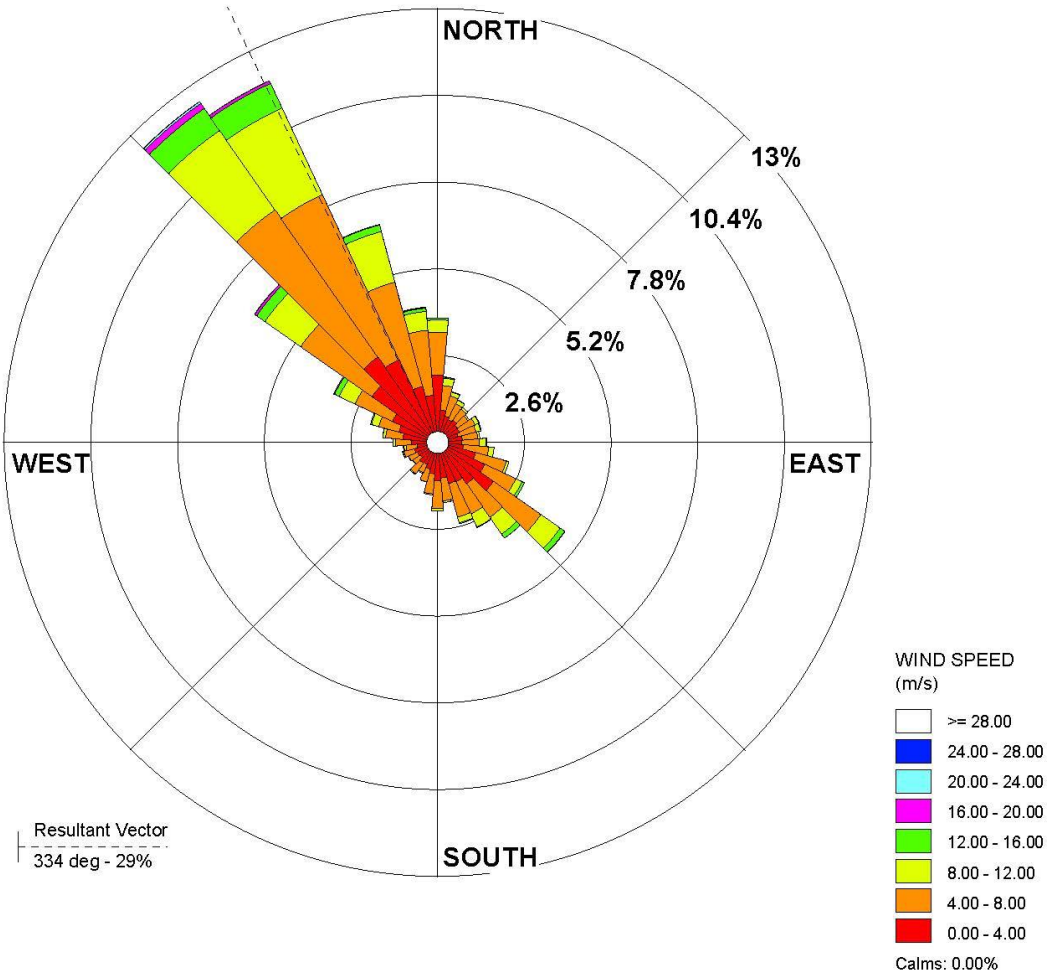

Figure 3.5: Wind rose for Meliadine site climate station.

3.2 Materials

Waste rock, waste overburden, and in situ overburden materials were all included in the modelling program. Waste rock material properties were assumed to be consistent with material observed at other Agnico Eagle sites in Nunavut. Specifically, material testing completed at the Portage WRSF located at the Meadowbank mine was used to approximate the texture, and therefore properties of the waste rock at Meliadine as very limited in situ sampling has been completed on run of mine waste rock at Meliadine. Okane (2021) compared a single run of mine waste rock sample from Meliadine to the samples collected at Meadowbank and found the single composite sample of Meliadine waste rock falls nearly within the range of waste rock texture sampled from the Portage WRSF and thus, is expected to be reasonably estimated by the material properties used in numerical modelling programs completed to date.

Waste overburden and in situ overburden properties were based on available drill sampling previously completed at Meliadine (Golder, 2012a; Golder, 2012b). All samples tested showed particle sizes no

larger than 76.2 mm. Overburden was generalized into finer-textured, coarser-textured, and average material types with average overburden used in modelling.

The material properties or functions developed for each material based on available geochemical and geotechnical testing (e.g., particle size distributions) are as follows:

- water retention curves (WRC – volumetric water content versus suction);
- hydraulic conductivity function (k-function – hydraulic conductivity versus suction);
- air conductivity function (air conductivity vs degree of saturation);
- thermal conductivity function (thermal conductivity versus volumetric water content);
- volumetric specific heat function (volumetric specific heat capacity versus volumetric water content);
- unfrozen water content function (unfrozen water content versus temperature); and
- geochemical reactivity.

Refer to Appendix A for a detailed description of material properties used in modelling.

3.3 Geometry

An idealized cross section was selected of WRSF8 for long term modelling (Figure 3.6). The cross section was selected as it was assumed to be the most representative of WRSF8 and WRSF9.

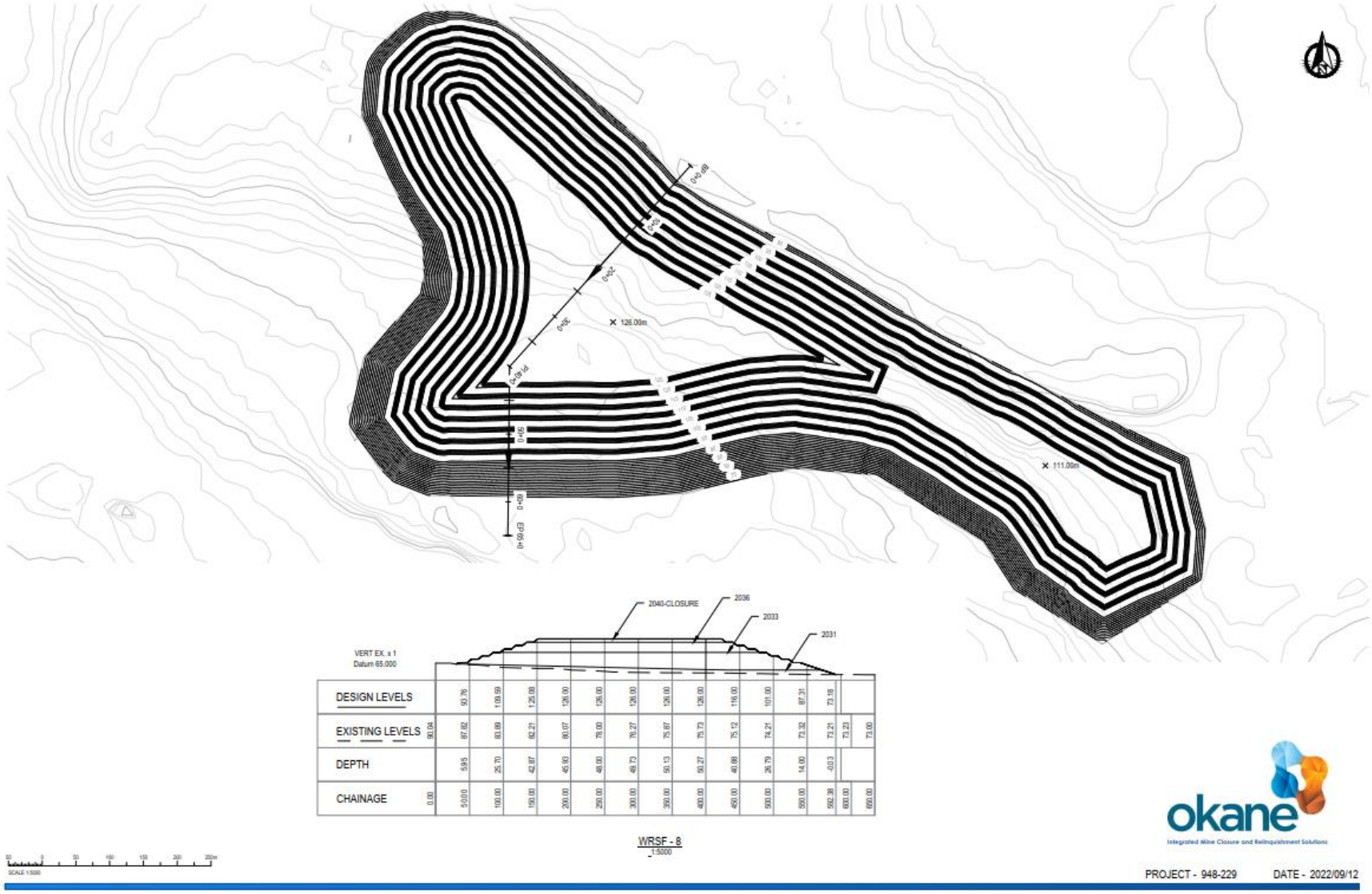

Figure 3.6: Location of idealized cross section used for modelling.

Typical geometry for the idealized cross-section is provided in Table 3.4 and Figure 3.7. This was 'built-up' over time in 2D to simulate conditions at placement (Appendix B). Previous thermal modelling work at Whale Tail and Meliadine showed the slope aspect had limited effect on the depth of thaw but that freeze-back would take longer along the southern aspects than the northern aspects. A southern exposure is expected to show conservative freeze-back through the WRSF due to increased solar radiation and less convective cooling from the leeward slope.

Table 3.4: Typical cross-section geometry for Discovery WRSF8.

Parameter	Idealized Cross Section
Initial Bench Height	5 m
Maximum Bench Height	5 m
Setback	10 m
Interbench Slope (Waste Rock)	1.3H:1V
Interbench Slope (Overburden)	1.8H:1V
Overall Slope (Ultimate toe to ultimate crest)	3.25H:1V
Cover Thickness	6 m

Timing of material placement (overburden) is expected to have a large impact on freeze-back time. It was assumed that the first lift of overburden is to be placed only in winter to maintain frozen conditions within the WRSF foundation materials.

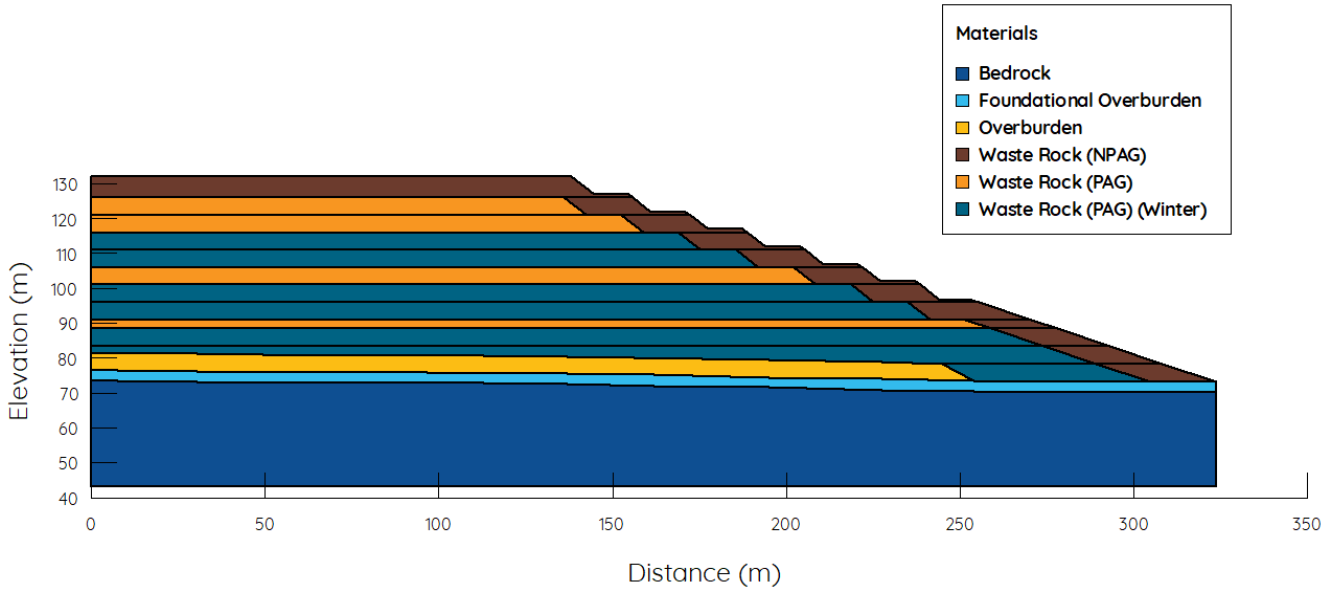

Figure 3.7: Idealized southwest facing cross-section of Meliadine Discovery WRSF8 (adapted from Tetra Tech, 2022).

3.4 Boundary Conditions

3.4.1 Hydraulic Boundary Conditions

The lower boundary was simulated as a unit hydraulic gradient. This boundary conditions assumes that at the lower boundary, the suction (and as a result, water content and hydraulic conductivity) are constant with depth. For this situation, the total head equals the gravitational head, which results in a unit hydraulic gradient. In other words, a unit hydraulic gradient represents a location in the material profile where water movement is controlled mainly by gravity.

3.4.2 Air and Gas Boundary Conditions

A barometric air pressure condition referenced to site elevation (75 masl) and adjusted for daily air temperature was applied to the exterior of the cross sections. A constant oxygen concentration representing atmospheric conditions (280 g/m^3) was also applied to the exterior of the cross sections.

3.4.3 Temperature Boundary Conditions

A depth of zero amplitude condition of -6 °C was assumed to exist at the base of the bedrock in the model geometry (approximately 30 mbgl) based on measured thermistor data in the footprint of the Discovery WRSFs (Figure 3.8).

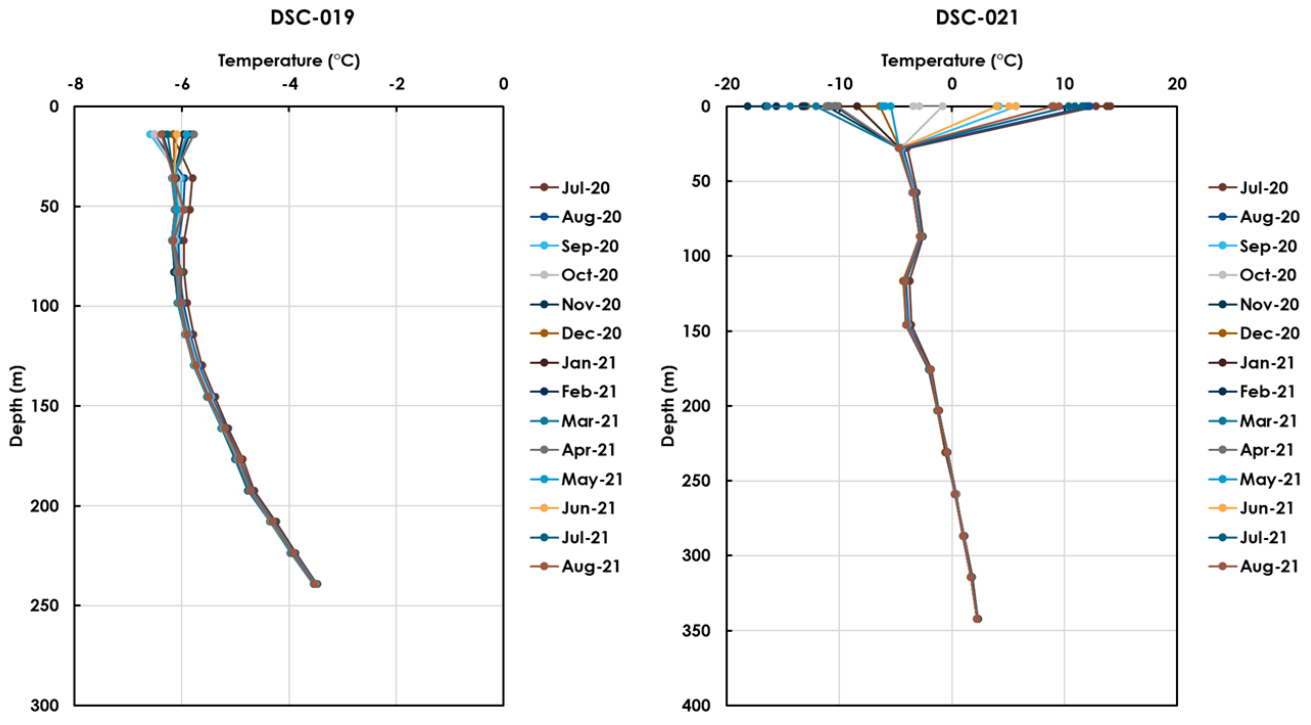

Figure 3.8: Bedrock temperatures measured within the footprint of the Discovery WRSFs.

Daily minimum and maximum temperature boundaries were applied to the exterior of the 2D cross section as described in Section 3.1.

3.5 Initial Conditions

Initial conditions for hydraulic, gas, and temperature conditions are required for modelling. The assumed initial conditions are summarized below (Table 3.5).

Table 3.5: Initial conditions used in numerical modelling simulations.

Parameter	Material	Value	Note
Temperature	Waste Rock	3 °C	Placed in summer
Temperature	Waste Rock / Overburden	-5 °C [1]	Placed in winter
Oxygen	Waste Rock / Overburden	280 g/m^3	Atmospheric
Air Pressure	Waste Rock / Overburden	0 kPa	Atmospheric
Volumetric Water Content	Waste Rock	0.05	
Volumetric Water Content	Overburden	0.2	

[1] Tetra Tech, 2019b.

4 MODEL RESULTS

Modelling of the Discovery WRSFs was completed in two major steps: one-dimensional soil-plant-atmosphere modelling and two-dimensional long-term modelling. One dimensional SPA modelling was completed to determine the surface water balance and surface temperature inputs for the 2D model. Models were completed for the base case climate change scenario (RCP4.5). The full climate database was applied to the Land-Climate-Interaction and Surface Energy Balance boundary conditions to determine the surface water balance and the surface temperature. The surface infiltration and surface temperature were then applied to the two-dimensional model.

Following completion of the one-dimensional models, long-term 2D modelling was completed to develop long-term thermal active layer depths, estimates of pore air temperature within the active layer, and a landform water balance. The long-term model was modelled for the time period for which a climate change model was developed (i.e. until 2120). As development of the Discovery WRSF is not expected to commence until 2031 the model encompassed a 90-year period (2031-2120). The modelling was completed under RCP4.5, including construction of the WRSF, using six-hour timesteps saved daily. The following sections summarize the results of the long-term 2D modelling.

4.1 Active Thermal Layer Depth

The long-term thermal modelling predicts permafrost at depth within the Discovery WRSFs and a shallow active layer that freezes and thaws every year. Figure 4.2 and Figure 4.3 illustrate the annual average near-surface thermal conditions for the Discovery WRSFs at several locations along the slope (Figure 4.1) between 2090-2120 under RCP4.5. The maximum depth of the freezing front in the winter is between 5 to 6 m over the last 30 years of modelling (2090-2120) at the Discovery WRSFs (Figure 4.2 and Figure 4.3).

In typical permafrost environments, thaw of the active layer occurs as a unidirectional process from surface, where the active layer absorbs and transfers heat from the atmosphere downwards toward the thawing front through conduction. Infiltrating water can contribute to the heat transfer through convection, however, thaw occurs primarily because of conduction of heat from the atmosphere.

Freezing in the autumn occurs first as a unidirectional process from the bottom of the active layer. As the ambient air temperature declines, the temperature gradient driving conduction also declines, resulting in freezing upwards from the permafrost. Once the air temperature becomes negative, a freezing front develops at the surface and progresses into the active layer, creating bidirectional freezing. The cold air temperatures rapidly cool the surficial material, allowing the freezing front to quickly progress downward, while the lower freezing front moves slowly upward. The thawed portion between the two freezing fronts is at or near 0 °C, creating isothermal or zero-curtain conditions, where water and ice can coexist in equilibrium. Unfrozen pore water migrates both upwards and downwards toward the freezing fronts until all pore water is frozen and the zero-curtain closes. The maximum depth of the active layer is reached when surface temperatures become negative and bidirectional freezing begins in October.

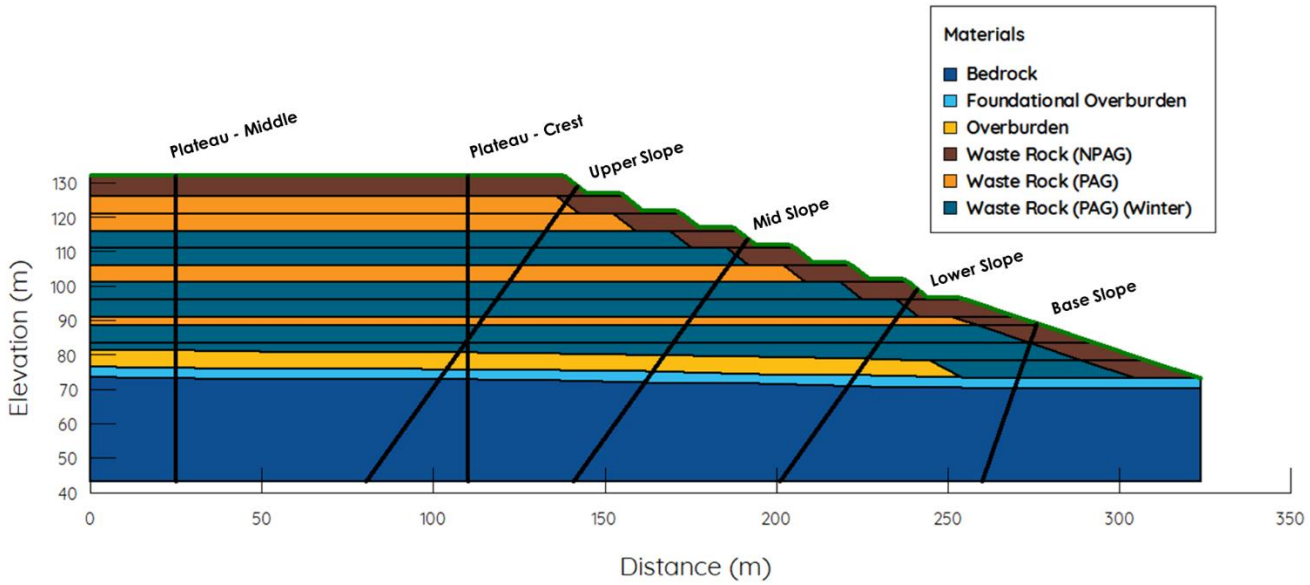

Figure 4.1: Section view of typical thermal locations rendered below.

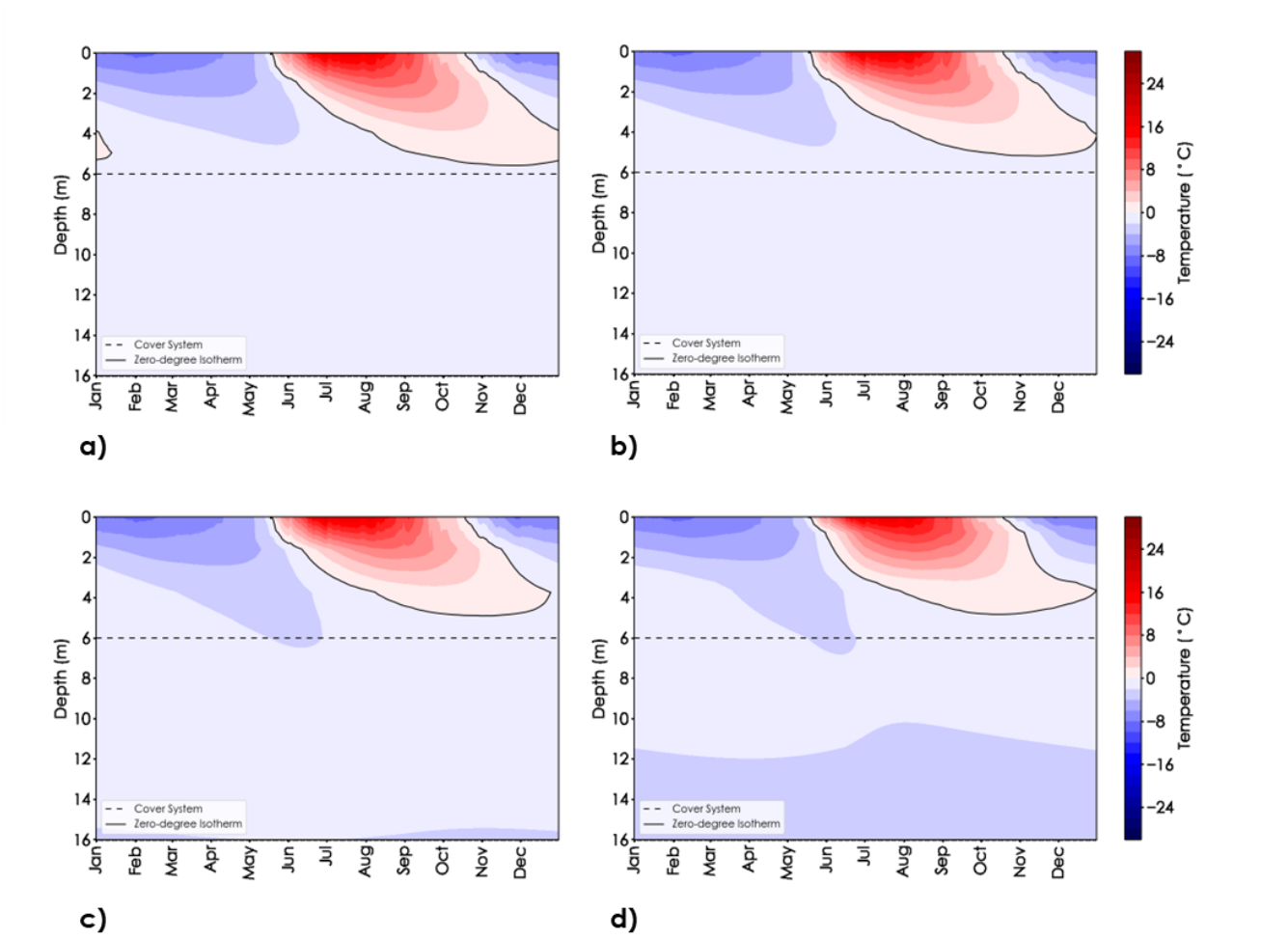

Figure 4.2: Annual long term near surface temperature along the slope of the Discovery WRSF model and the a) upper slope, b) mid slope, c) lower slope, and d) base slope profile under RCP4.5 climate conditions with the proposed cover system interface shown by the black dashed line.

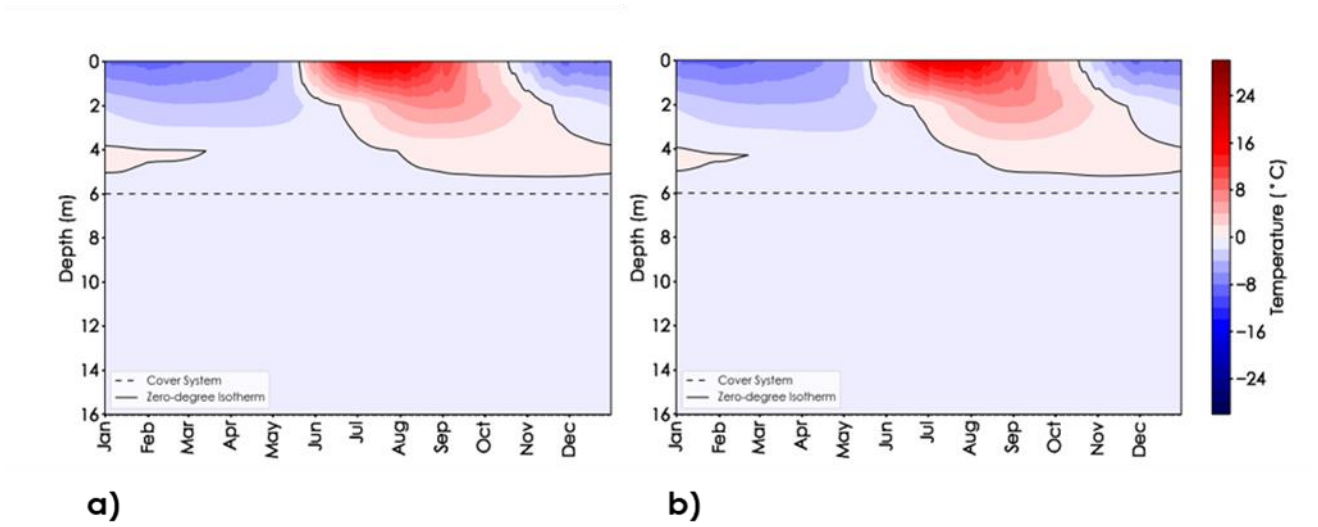

Figure 4.3: Annual long term near surface temperature along the plateau of the Discovery WRSF model and the a) middle, and b) crest under RCP4.5 climate conditions with the proposed cover system interface shown by the black dashed line.

Internal heating from oxidation of sulfidic materials (PAG waste rock) at the Discovery WRSFs provides an additional source of heat within the WRSFs that contributes warmer internal temperatures but is not enough to cause thaw.

4.2 Active Layer Temperature Profile

Waste rock temperature is required to estimate reaction rates and loading rates from the WRSFs. Detailed temperature profile results of the mid-slope location by month and depth are summarized in Appendix C.

4.3 Landform Water Balance

A landform water balance was completed to aid in the thermal modelling. This work includes estimates of runoff, interflow and basal seepage rates. A summary of the surface water balance for the WRSF plateau and slope is provided in Table 4.1 for the long-term model under RCP4.5.

Table 4.1: Summary of average water balance for the plateau and slope of the long-term model under RCP4.5 conditions (2051-2120*).

Water Balance Parameters	RCP4.5	
	Plateau	Slope
Total Precipitation (mm)	465 mm	465 mm
Rainfall (% of Total Precipitation)	55-60%	55-60%
Snow (% of Total Precipitation)	40-45%	40-45%
Actual Evaporation (% of Total Precipitation)	40-45%	40-45%
Runoff (% of Total Precipitation)	1-5%	1-5%
Surface Infiltration (% of Total Precipitation)	15-20%	15-20%
Sublimation (% of Total Precipitation)	30-35%	30-35%

* Water balance results are reported for the post-closure period to illustrate long-term trends.

Runoff is assumed to interact with surficial materials to a depth of 30 cm (Sharpely, 1985; Zhang, 2009). Table 4.2 summarizes the runoff distribution by month for the Discovery WRSFs.

Table 4.2: Runoff distribution by month for the Discovery WRSFs under RCP4.5 (2051-2120*).

Month	RCP4.5	
	Plateau	Slope
January	0%	0%
February	0%	0%
March	0%	0%
April	28%	28%
May	71%	72%
June	1%	0%
July	0%	0%
August	0%	0%
September	0%	0%
October	0%	0%
November	0%	0%
December	0%	0%

* Water balance results are reported for the post-closure period to illustrate long-term trends.

4.3.1.1 Basal Seepage

The high infiltration capacity of the waste rock material results in a propensity for incident precipitation to become surface infiltration, rather than runoff (Table 4.1). As water infiltrates into the surficial materials, net percolation flows vertically through the WRSF, eventually freezing back at depth. The base layer of

the Discovery WRSFs is consistently frozen from the time of placement. As a result, basal seepage from the landform is negligible.

4.3.1.2 Interflow

Interflow occurs as lateral flow within the active layer on the plateaus and slopes. During construction and freeze back, water can percolate into the Discovery WRSFs beyond the active layer, resulting in increased storage and consequently lower interflow. As time progresses, a zone of high saturation, ice-rich frozen waste rock develops below the active layer and prevents further percolation, resulting in the lateral diversion of infiltrating water and greater interflow.

Table 4.3 shows the progression of interflow with time as a percent of total precipitation for the Discovery WRSFs. The monthly distribution of interflow is shown in Table 4.4 for the Discovery WRSFs.

Table 4.3: Interflow for the Discovery WRSFs cross section as a percent of total precipitation (2051-2120*).

	RCP4.5	
	2051-2090	**2091-2120**
Interflow (% of Total Precipitation)	10-15%	15-20%

* Water balance results are reported for the post-closure period to illustrate long-term trends.

Table 4.4: Interflow distribution by month for the Discovery WRSFs cross section as a percent of total interflow (2051-2120*).

Month	**Percent of Interflow Occurring by Month (RCP4.5)**	
	2051-2090	**2091-2120**
January	0%	0%
February	0%	0%
March	0%	0%
April	0%	0%
May	5%	6%
June	12%	11%
July	15%	14%
August	19%	20%
September	27%	24%
October	18%	19%
November	3%	5%
December	<1%	<1%

* Water balance results are reported for the post-closure period to illustrate long-term trends.

5 CONCLUSIONS

The thermal modelling of the proposed Meliadine Discovery WRSFs presented herein is intended to provide long-term hydrologic and thermal inputs for the site-wide water and load balances, as well as a basis for closure design of the WRSFs which is defendable to internal project stakeholders and regulators by addressing material risk to the project related to the WRSFs. Long term thermal models were completed for long term climate models RCP4.5 to assess the potential effects of climate change on geochemical loading.

The active layer is anticipated to be approximately 5 to 6 m and thus will be contained within the 6 m NPAG/NML cover system. As such the PAG/ML material will remain frozen, limiting the potential loading pathway to the NPAG/NML.

The major component of the surface water balance which has the potential to result in geochemical loading from the WRSF is surface infiltration that results in interflow. Runoff and basal seepage are expected to be nearly negligible. In the idealized cross section modelling, representative of the Discovery WRSFs, where most of the waste rock is expected to be PAG/ML, this potential loading pathway is limited to the NPAG/NML materials.

6 REFERENCES

Agnico Eagle Mines Limited - Meliadine Division (Agnico Eagle). 2022. Meliadine Mine – Meliadine Extension FEIS Addendum. July 26, 2022.

Agnico Eagle Mines Limited – Meadowbank Division (Agnico Eagle). 2019. Final Written Statement Responses Whale Tail Pit – Expansion Project. Submitted to Nunavut Impact Review Board August 9, 2019.

Agnico Eagle Mines Limited (Agnico Eagle). 2020. Agnico Eagle Meliadine Division PLOM 2021 Surface Layout. Figure 1 RevA.

Black, P.B. and Tice, A.R. 1989. Comparison of soil freezing curve and soil water curve data for Windsor Sandy Loam. Water Resources Research. 25(10):2205-2210.

Canadian Climate Data and Scenarios (CCDS). 2018. Online. http://climate-scenarios.canada.ca/

Environment and Climate Change Canada. 2016. Canadian Weather Energy and Engineering Datasets (CWEEDS). Online. https://climate.weather.gc.ca/prods_servs/engineering_e.html

Environment and Climate Change Canada. 2017. Adjusted daily rainfall and snowfall dataset for Canada. Online. https://open.canada.ca/data/en/dataset/d8616c52-a812-44ad-8754-7bcc0d8de305

Environment and Climate Change Canada. 2020. Data for Rankin Inlet. Online. http://climate.weather.gc.ca/index_e.html

Fredlund, D.G., Rahardjo, H., and Fredlund, M.D. 2012. Unsaturated Soil Mechanics in Engineering Practice. John Wiley & Sons, Inc.

Golder Associates (Golder). 2012a. SD 2-4A Factual Report on 2011 Geotechnical Drilling Program – Meliadine Gold Project, Nunavut.

Golder Associates (Golder). 2012b. SD 2-4B Factual Report on 2012 Geotechnical Drilling Program – Meliadine Gold Project, Nunavut.

Golder Associates (Golder). 2014a. Meliadine FEIS – SD 6-3 Geochemcial Characterization of Waste Rock, Ore, Tailings, and Overburden - Meliadine Gold Project, Nunavut. Prepared for Mines Agnico Eagle. April 2014.

Golder Associates (Golder). 2014b. Meliadine FEIS – SD 2-17 Preliminary Mine Closure and Reclamation Plan – Meliadine Gold Project, Nunavut. Prepared for Agnico Eagle Mines Limited. April 2014.

International Network for Acid Prevention (INAP). 2017. Global Cover System Design Technical Guidance Document. November 2017.

IPCC. 2013. Climate Change 2013: The Physical Science Basis. Contribution of Working Group I to the Fifth Assessment Report of the Intergovernmental Panel on Climate Change. Stocker, T.F., D. Qin, G.-K. Plattner, M. Tignor, S.K. Allen, J. Boschung, A. Nauels, Y. Xia, V. Bex and P.M. Midgley (eds.). Cambridge University Press. Cambridge, United Kingdom and New York, NY, USA.

Lorax. 2022. Meliadine Extension: Geochemical Characterization and Source Term Report. Prepared for Agnico Eagle Mines Ltd., by Lorax Environmental Services, February 2022.

Meinshausen, M., S. J. Smith, K. V. Calvin, J. S. Daniel, M. L. T. Kainuma, J.-F. Lamarque, K. Matsumoto, S. A. Montzka, S. C. B. Raper, K. Riahi, A. M. Thomson, G. J. M. Velders and D. van Vuuren. 2011. The RCP Greenhouse Gas Concentrations and their Extension from 1765 to 2300. Climatic Change (Special Issue), DOI: 10.1007/s10584-011-0156-z.

Okane Consultants Inc. (Okane). 2021. Particle Size Distribution Analysis of Sampled Waste Rock at Meliadine WRSFs. 948-021-009 Rev0. Prepared for Agnico Eagle Mines Limited. January 2021.

Okane Consultants Inc. (Okane). 2020. Meliadine Waste Rock Storage Facility Failure Modes and Effect Analysis. 948-021-002 Rev 0. Prepared for Agnico Eagle Mines Limited. March 2020.

Pacific Climate Impacts Consortium (PCIC). 2018. Online. https://pacificclimate.org/

Peacock, S. 2012. Projected Twenty-First-Century Changes in Temperature, Precipitation, and Snow Cover over North America in CCSM4. Journal of Climate. 25. pp. 4406-4429

Pham, N.H., Amos, R., Blowes, D., Smith, L., and Sego, D. 2015. The Diavik Waste Rock Project: Heat transfer in a large scale waste rock pile constructed in a permafrost region. Proceedings of the 10th International Conference on Acid Rock Drainage & IMWA Annual Conference. Santiago, Chile. April 21-24, 2015.

Pham, NH, Sego, DC, Arenson, LU, Blowes, DW, Amos, RT and Smith, L. 2013. The Diavik Waste Rock Project: Measurement of the thermal regime of a waste-rock pile in a permafrost environment. In Applied Geochemistry Volume 36, September 2013,m Pages 234-245.

Rubel, F., and M. Kottek, 2010: Observed and projected climate shifts 1901-2100 depicted by world maps of the Köppen-Geiger climate classification. Meteorol. Z., 19, 135-141.

Sharpley, A. (1985). Depth of surface soil-runoff interaction as affected by rainfall, soil slope, and management. *Soil Science Society of America Journal, 49*(4), 1010-1015.

Swift, L.W.Jr.. 1976. Algorithm for Solar Radiation on Mountain Slopes. Water Resources Research Vol. 12, No. 1.

Tetra Tech Canada Inc. (Tetra Tech). 2022. Agnico Eagle Meliadine Extension WRSF Plan and Sections. Drawing Nos. WRSF5 Rev A & WRSF8 Rev A.

Tetra Tech Canada Inc. (Tetra Tech). 2021. Rankin Inlet Extended Adjusted Daily Precipitation Data.xlsx. May 2021.

Tetra Tech Canada Inc. (Tetra Tech). 2019a. Alternative Assessment on Waste and Water Management, Meliadine Gold Project Phase II Extension, Meliadine, Nunavut, Canada. Prepared for Agnico Eagle, November 2019.

Tetra Tech Canada Inc. (Tetra Tech). 2019b. Thermal Analyses for Waste Rock Storage Facility No1 (WRSF1), Meliadine Project, Nunavut.

van Vuuren, D.P., Edmonds, J., Kainuma, M., Raihi, K., Thomson, A., Hibbard, K. Hurtt, G.C., Kram, T. Krey, V., Lamarque, J.F., et al. 2011. The representative concentration pathways: an overview. Climatic Change. Vol. 109.

Weeks, B. and Wilson, G.W. 2006. Prediction of evaporation from soil slopes. Canadian Geotechnical Journal Vol. 43.

Wilby, R.L., Dawson, C.W. Murphy, C. O'Conner, P., and Hawkins, E. 2014. The Statistical DownScaling Model – Decision Centric (SDSM-DC): Conceptual basis and applications. Climate Research, 61, 251-268.

Wilby, R.L. and Dawson, C.W. 2013. The Statistical DownScaling Model (SDSM): Insights from one decade of application. International Journal of Climatology, 33, 1707-1719.

Wilby, R.L., Dawson, C.W. and Barrow, E.M. 2002. SDSM – a decision support tool for the assessment of regional climate change impacts. Environmental and Modelling Software, 17, 145-157.

Zhang, Y., & Zhang, X. 2009. Experimental analysis of the effective depth of interaction of rainfall - Surface runoff - Soil nitrogen.

Appendix A

Material Properties

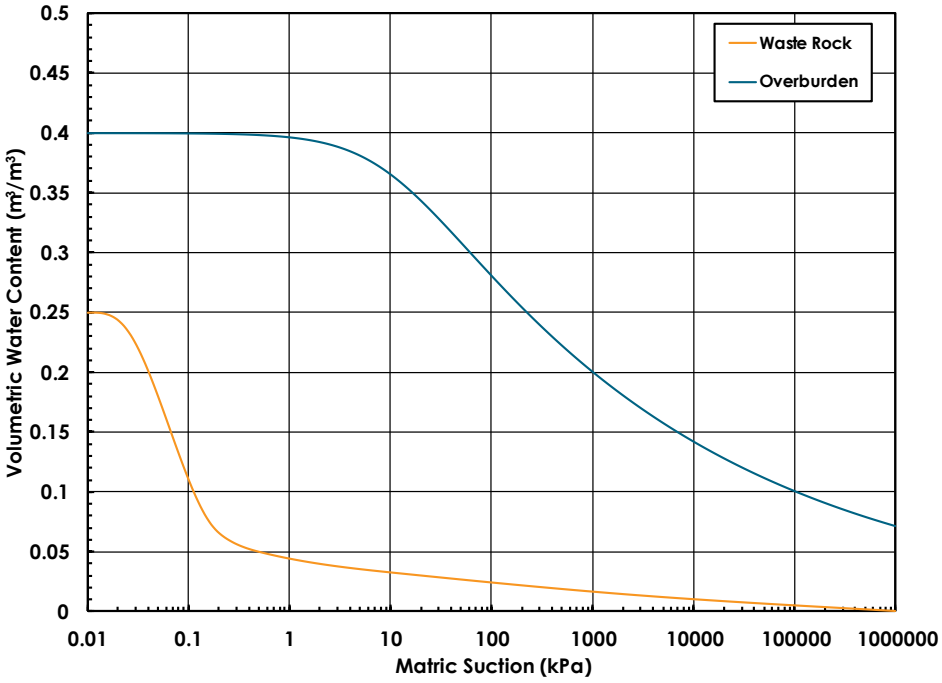

Figure A.1: Water retention curves estimated for the overburden and waste rock materials.

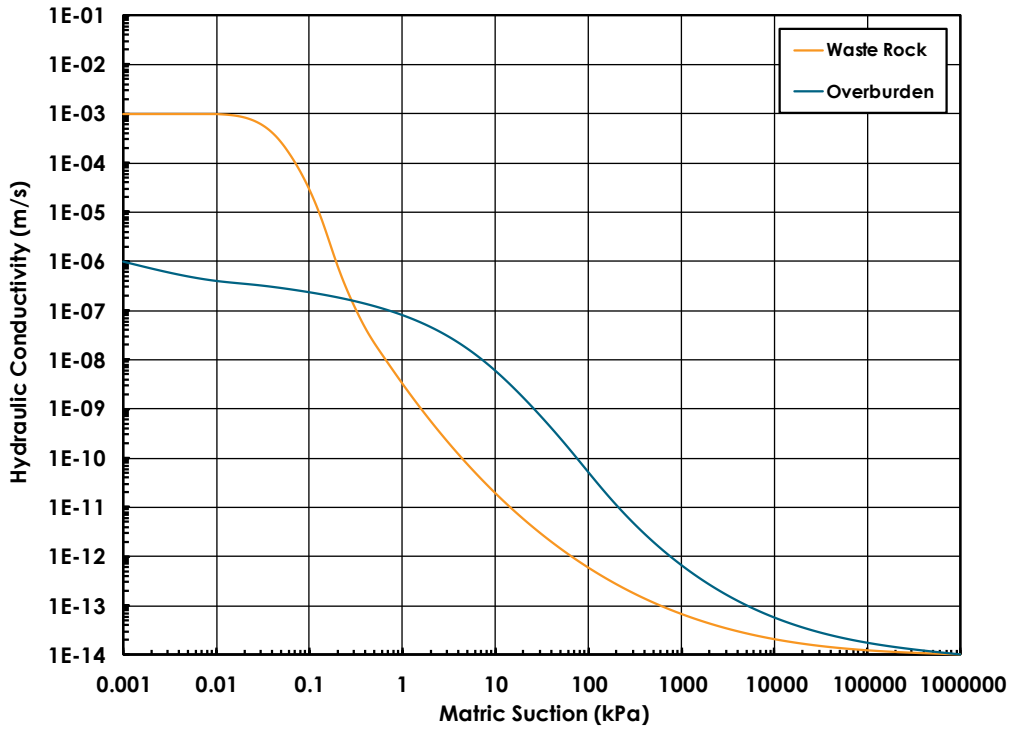

Figure A.2: Hydraulic conductivity functions estimated for the overburden and waste rock materials.

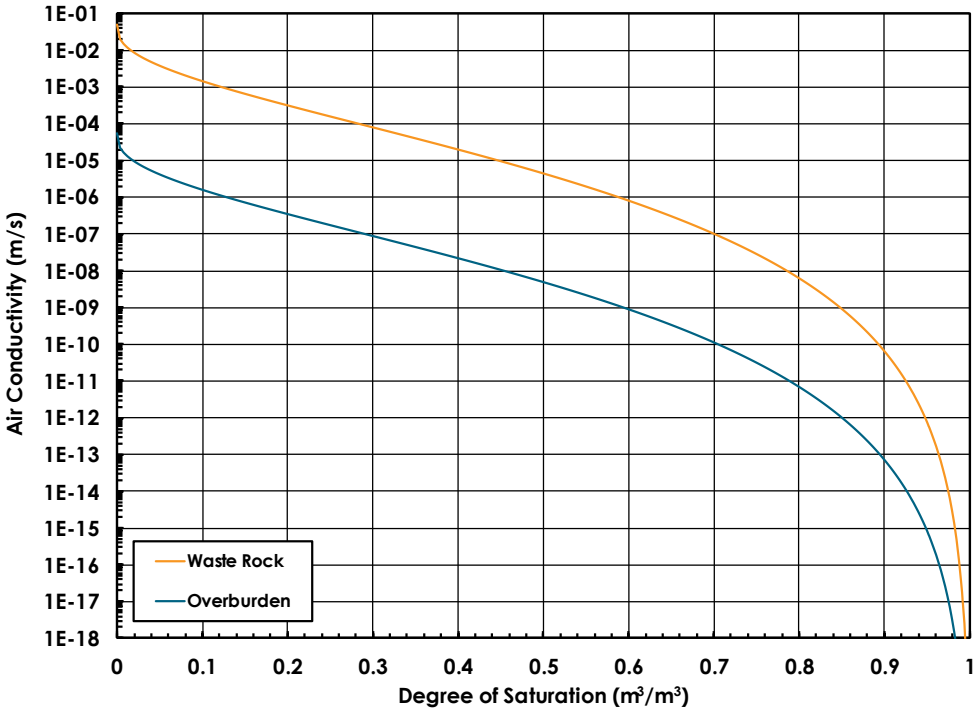

Figure A.3: Air conductivity functions estimated for the overburden and waste rock materials.

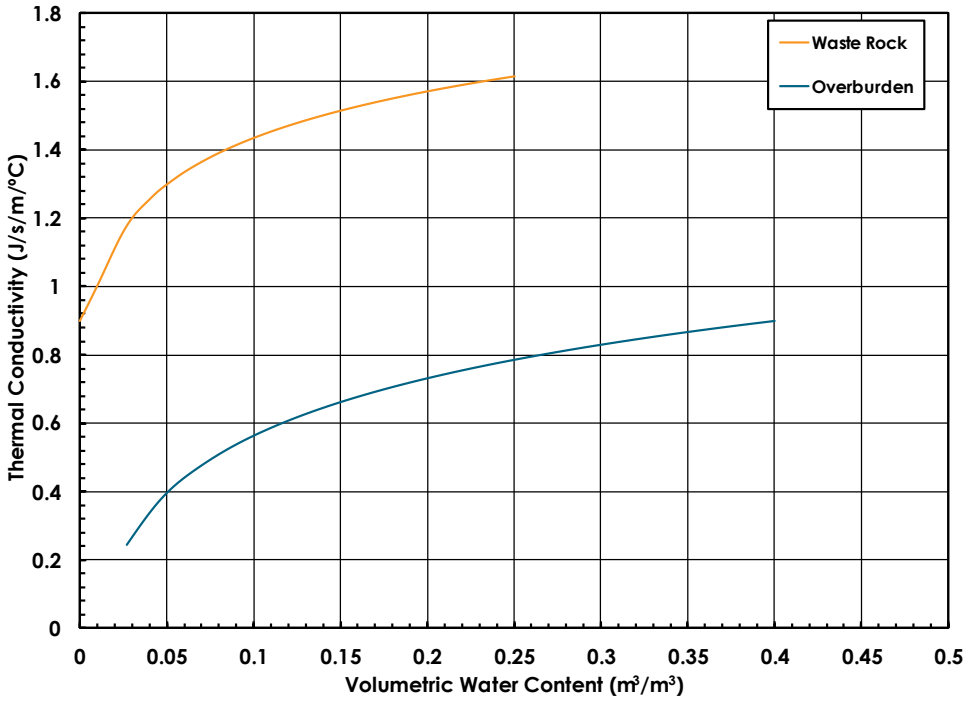

Figure A.4: Thermal conductivity functions estimated for the overburden and waste rock materials.

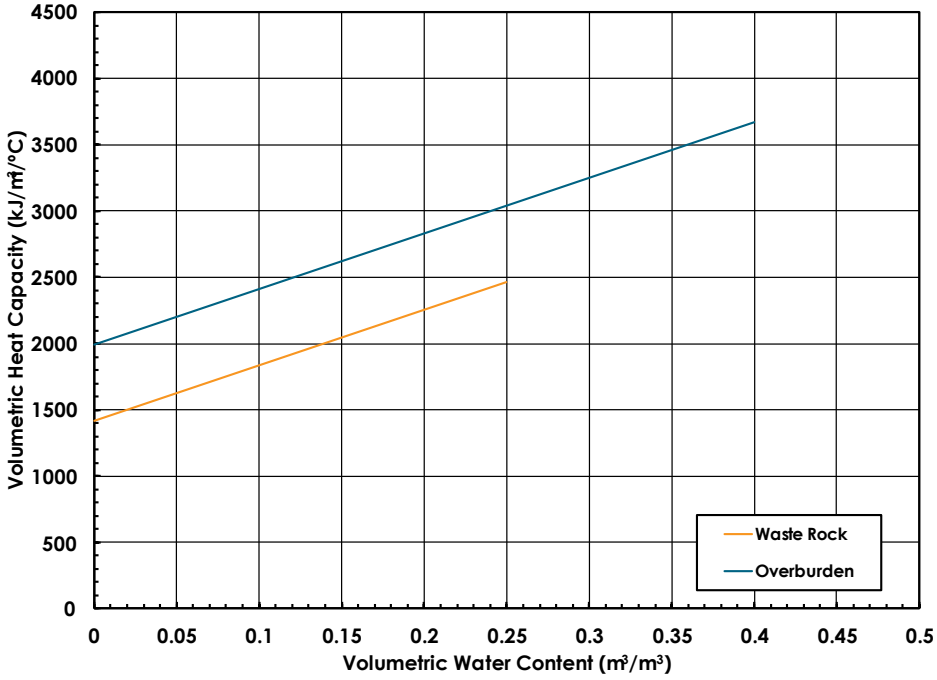

Figure A.5: Volumetric heat capacity functions estimated for the overburden and waste rock materials.

Appendix B

Model Geometry Evolution

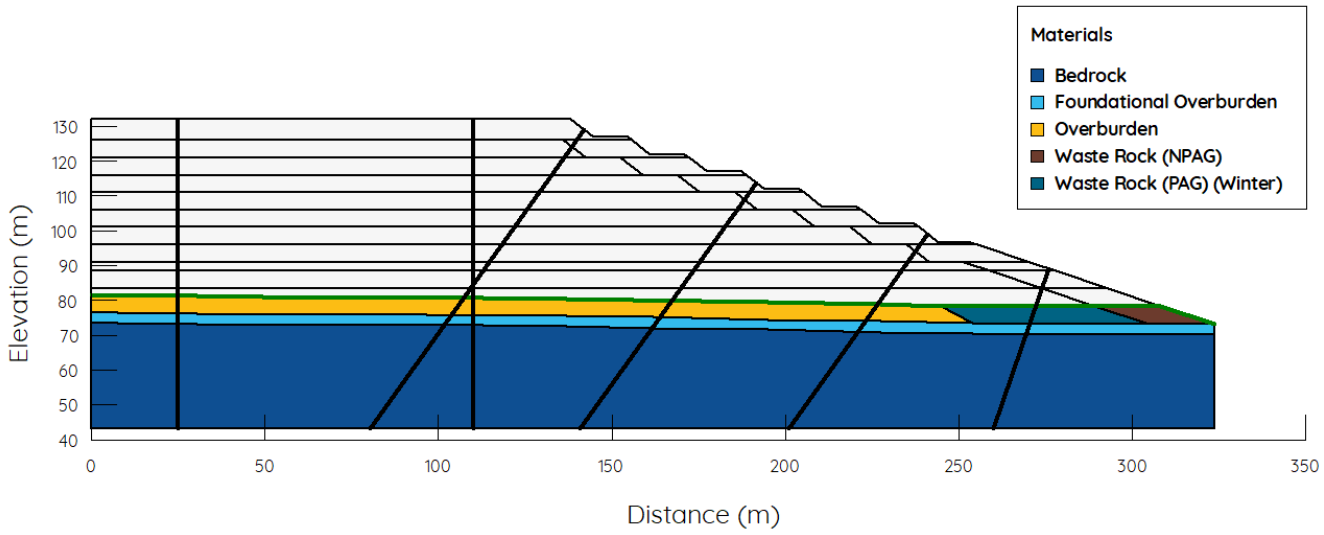

Figure B.1: Meliadine Discovery WRSF construction – Winter 2031.

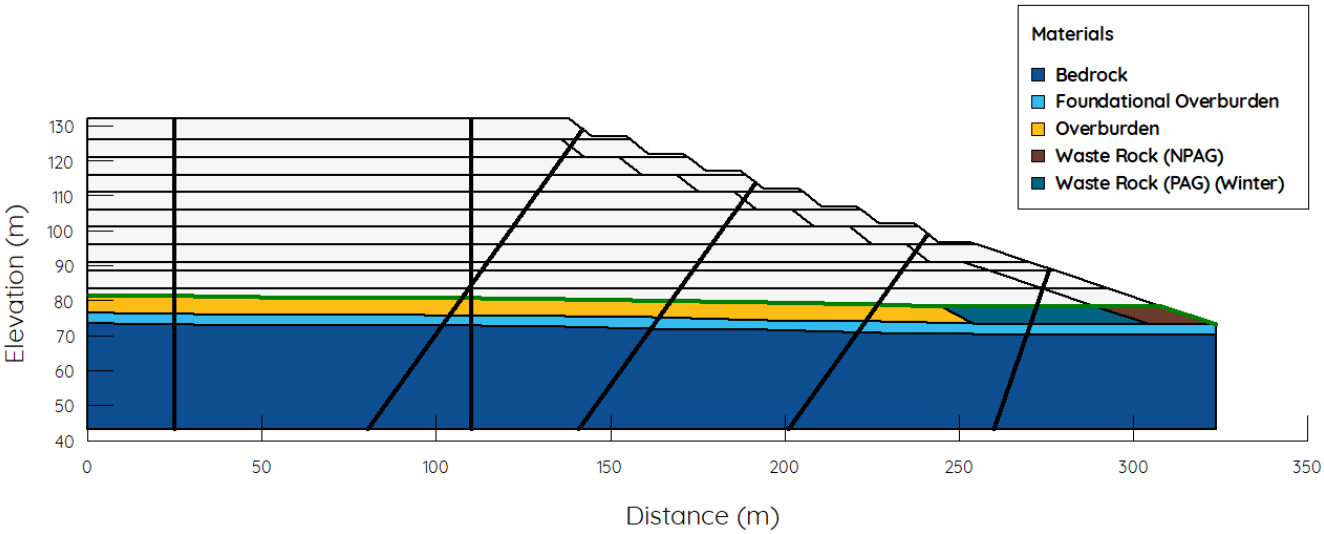

Figure B.2: Meliadine Discovery WRSF construction – Summer 2031.

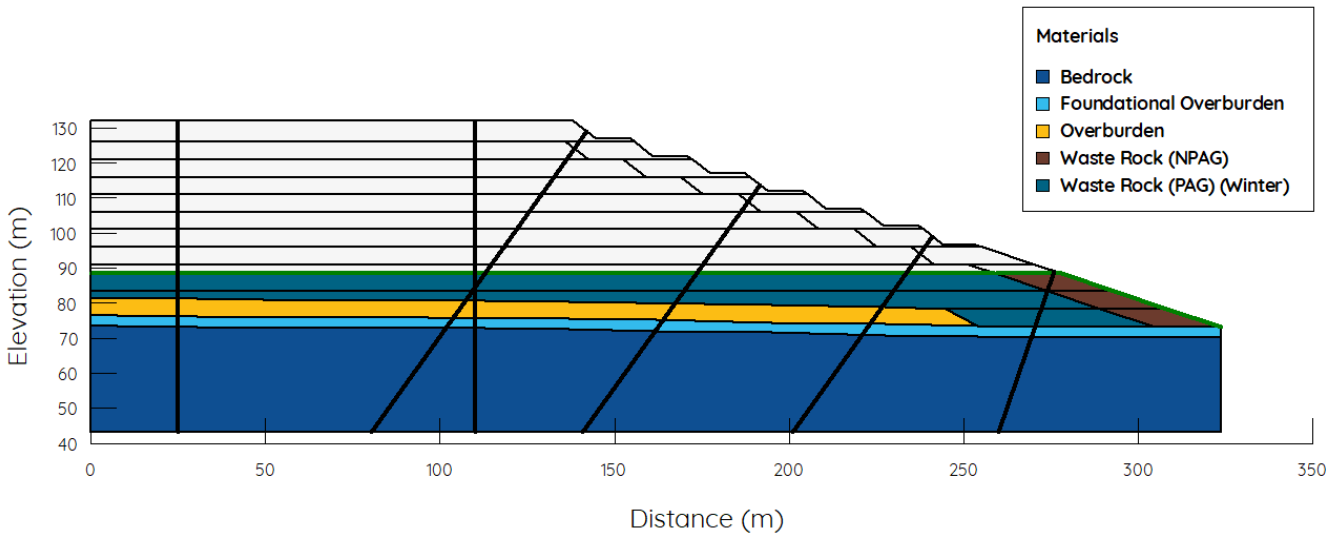

Figure B.3: Meliadine Discovery WRSF construction – Winter 2032.

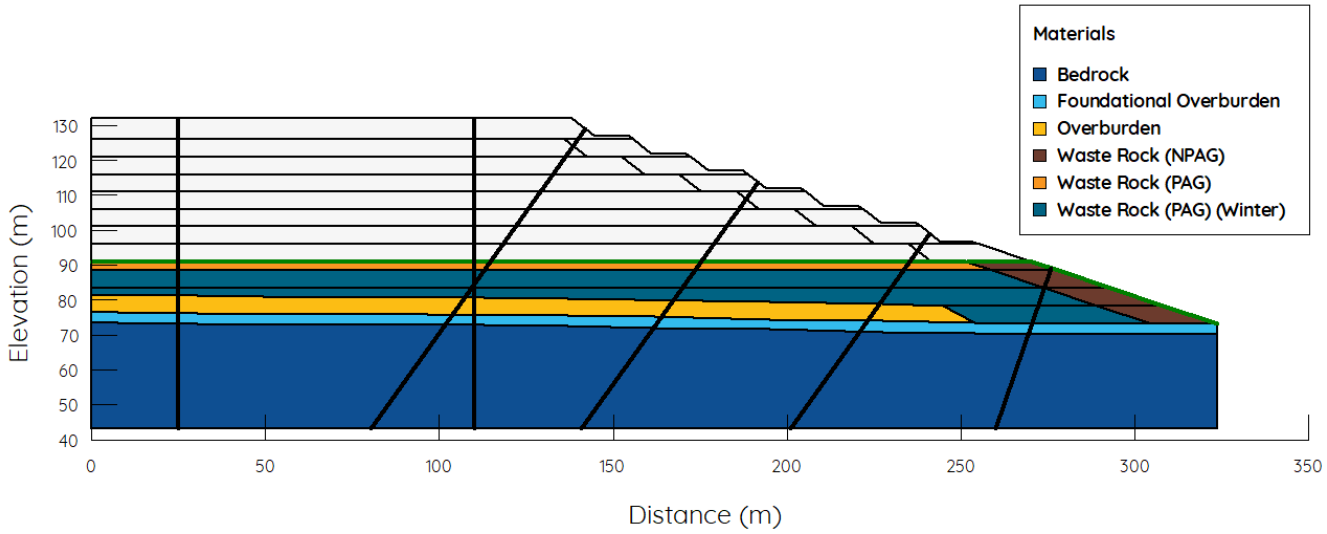

Figure B.4: Meliadine Discovery WRSF construction – Summer 2032.

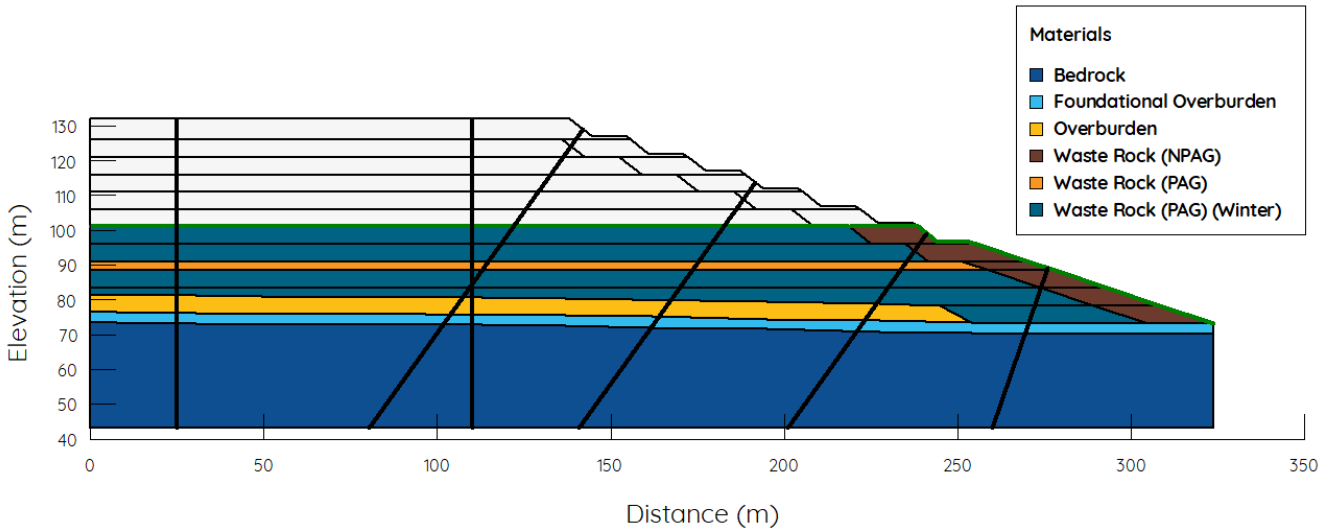

Figure B.5: Meliadine Discovery WRSF construction – Winter 2033.

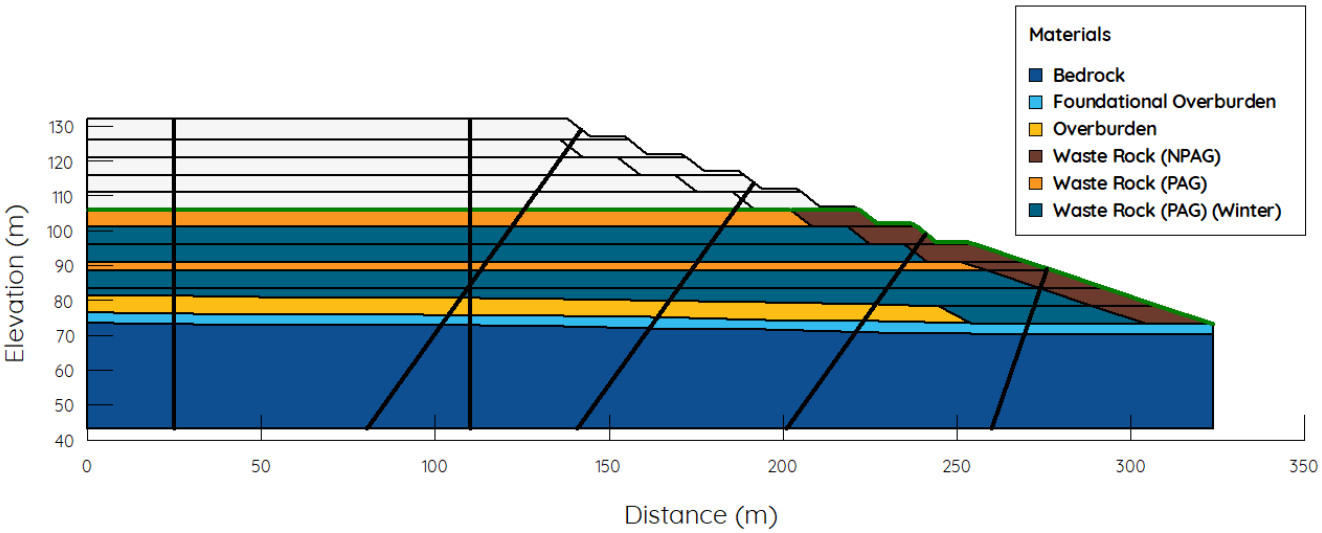

Figure B.6: Meliadine Discovery WRSF construction – Summer 2033.

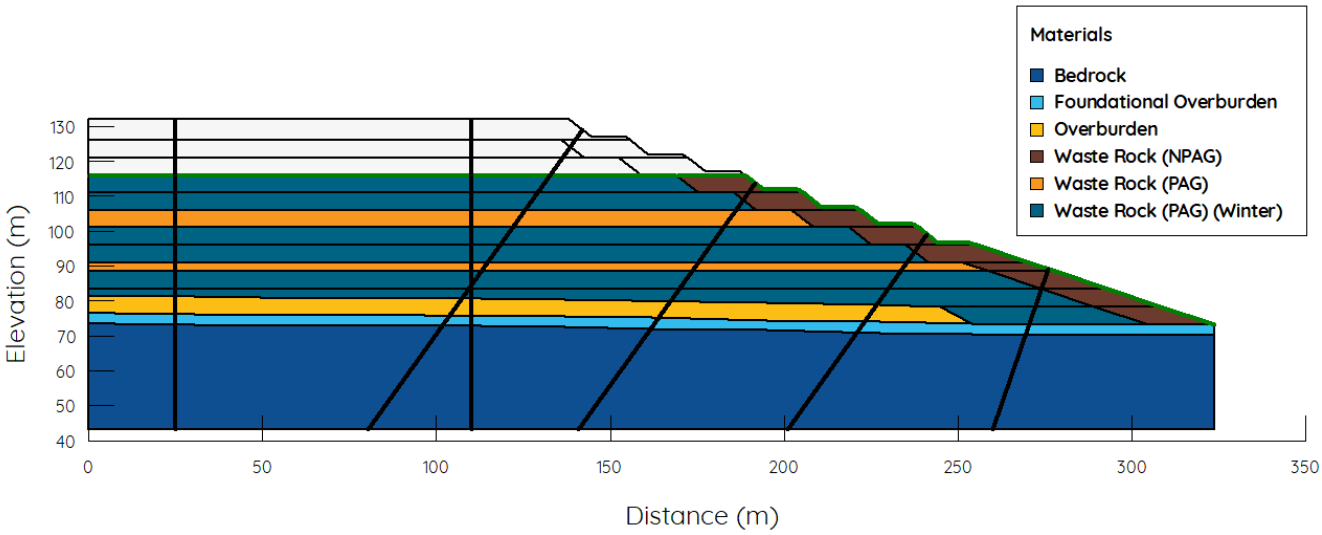

Figure B.7: Meliadine Discovery WRSF construction – Winter 2034.

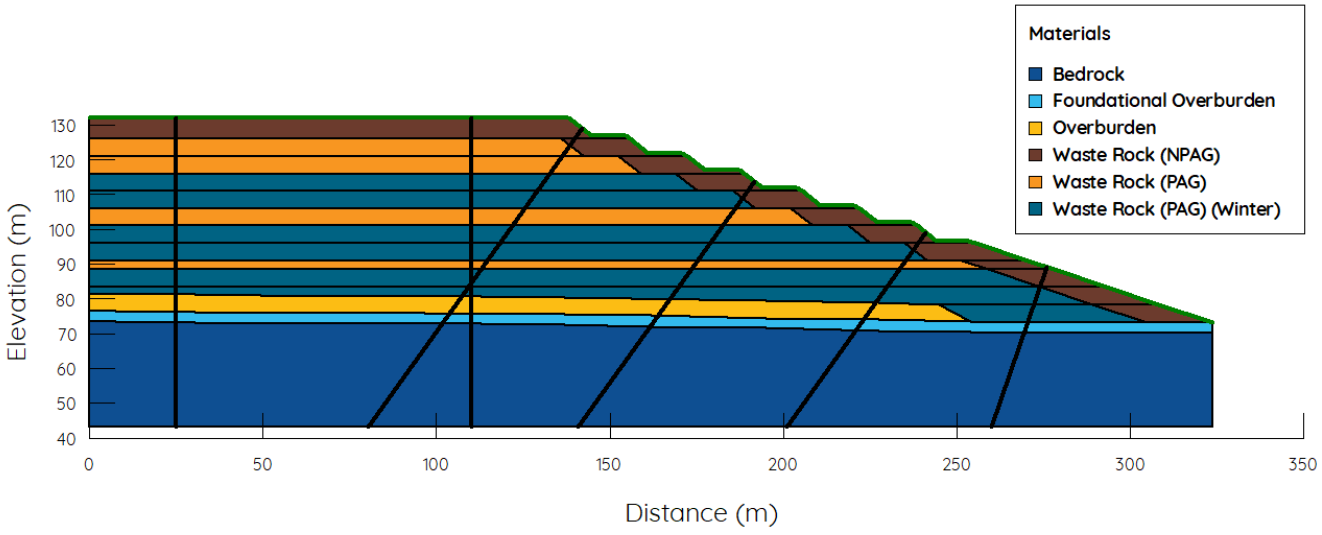

Figure B.8: Meliadine Discovery WRSF construction – Summer 2034.

Appendix C

WRSF Temperature Profiles

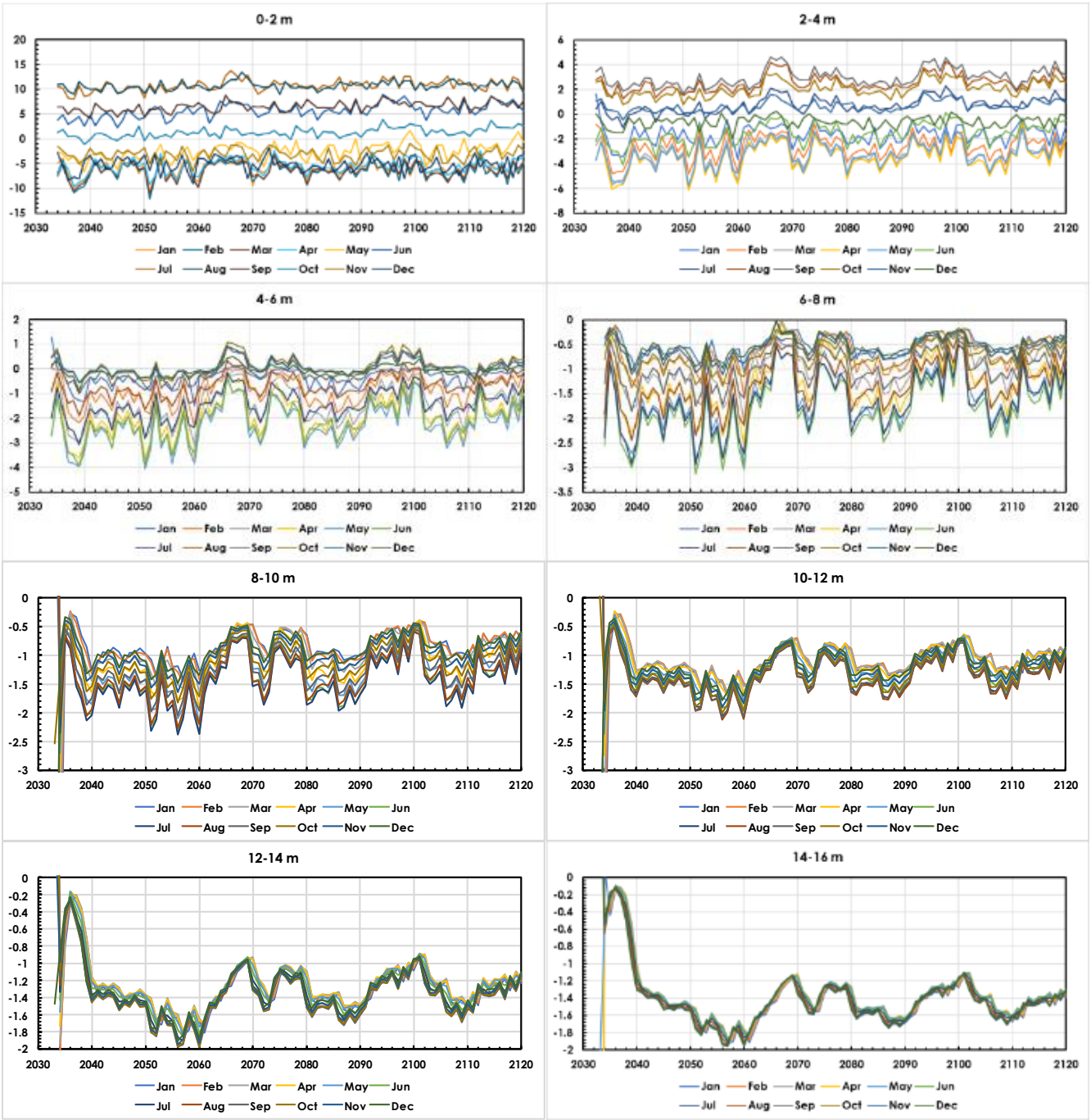

Figure C.1: Thermal profiles for RCP4.5 for the mid-slope profile (°C).

For further information contact:

Gillian Allen
Senior Engineer
gallen@okc-sk.com

Okane Consultants Inc.

112 - 112 Research Drive
Saskatoon, SK S7N 3R3
Canada

Telephone: (306) 955 0702
Facsimile: (306) 955 1596
Web: www.okc-sk.com